Electronic Research Archive

http://www.aimspress.com/journal/era

ERA, 34(5): 3410–3446.
DOI: 10.3934/era.2026153
Received: 27 February 2026
Revised: 13 April 2026
Accepted: 17 April 2026
Published: 22 April 2026

Research article

A robust weak Galerkin method for singularly perturbed fourth-order convection–diffusion problems

Suayip Toprakseven[1,*] **and Seza Dinibutun**[2]

[1] Department of Mathematics, Faculty of Art and Science, Yozgat Bozok University, Yozgat 66100, Türkiye
[2] Department of Mathematics and Natural Sciences, International University of Science and Technology in Kuwait, Ardiya 92400, Kuwait

* **Correspondence:** Email: topraksp@artvin.edu.tr.

Abstract: We propose a uniform weak Galerkin finite element method (WG-FEM) to solve singularly perturbed fourth-order convection–diffusion problems exhibiting boundary layers. The method is designed to handle small perturbation parameters ε, ensuring accurate resolution of sharp layers without spurious oscillations. We construct appropriate layer-adapted meshes and use uniform estimates to analyze the stability and convergence of the weak Galerkin scheme. Numerical experiments confirm the theoretical results and demonstrate that the method achieves uniform convergence with respect to the perturbation parameter, effectively capturing the boundary layer behavior on layer-adapted meshes. The proposed approach provides a reliable and efficient tool for high-order singularly perturbed problems with mixed derivative boundary conditions.

Keywords: weak Galerkin method; singularly perturbed problems; fourth-order convection-diffusion; boundary layers; uniform convergence; layer-adapted meshes

1. Introduction

In this paper, we analyze a weak Galerkin finite element method (WG-FEM) for a class of singularly perturbed fourth-order boundary value problems of the form

$$\varepsilon v^{(4)}(x) - \left(\kappa(x)v''(x)\right)' - \left(\eta(x)v'(x)\right)' + \rho(x)v'(x) + \sigma(x)v(x) = h(x) \text{ in } \Omega, \tag{1a}$$

$$v(0) = \gamma_0, \quad v(1) = \gamma_1, \quad v'(0) = \zeta_0, \quad v''(1) = \zeta_1, \tag{1b}$$

where $\Omega := (0, 1)$ and $0 < \varepsilon \ll 1$ is a small perturbation parameter.

Throughout the paper, we assume that the coefficient functions $\kappa(x)$, $\eta(x)$, $\rho(x)$, $\sigma(x)$, and the source term $h(x)$ are sufficiently smooth on $[0, 1]$. Moreover, positive constants κ_0, η_0, and σ_0 exist such that

$$\kappa(x) \geq \kappa_0 > 0, \quad \eta(x) - \tfrac{1}{2}\kappa'(x) \geq \eta_0 > 0, \quad \sigma(x) - \tfrac{1}{2}\rho'(x) \geq \sigma_0 > 0, \quad x \in \Omega. \tag{2}$$

We remark that the inclusion of lower-order convective terms does not affect the essential structure of the analysis. The chosen boundary conditions allow the derivation of parameter-uniform stability estimates and improve the regularity properties of the exact solution. Other types of boundary conditions can also be treated within the proposed WG-FEM framework.

Singularly perturbed fourth-order problems of this type arise in various applications, including beam and plate models in structural mechanics, as well as viscoelastic flow problems. Due to the presence of the small parameter ε, solutions typically exhibit boundary layers in higher-order derivatives. In particular, sharp gradients may appear near $x = 1$, with a layer thickness of order $O(\varepsilon \ln(1/\varepsilon))$, which presents significant challenges for classical numerical methods.

Setting $\varepsilon = 0$ reduces the differential order of the problem, leading to a degenerate limit equation. This structure motivates classifying the model as a convection–diffusion type problem in a higher-order setting. Although it shares similarities with classical second-order singularly perturbed convection–diffusion equations, the present problem exhibits more complex layer behavior due to the fourth-order derivative terms.

Singularly perturbed second-order problems have been extensively studied; see, for example, [1–3]. However, significantly fewer results are available for fourth-order cases. Early contributions include Semper [4], who analyzed C^1 finite element approximations on quasi-uniform meshes. Uniform convergence on layer-adapted Shishkin meshes for higher-order elliptic problems was established in [5]. Superconvergence properties on modified Shishkin meshes were studied in [6]. Further developments include nonconforming methods such as the Adini element analysis of Meng and Stynes [7], and mixed finite element error estimates in energy and balanced norms were addressed by Franz and Roos [8].

Most existing analytical and numerical investigations of singularly perturbed fourth-order problems have predominantly concentrated on equations of the reaction–diffusion type [9]. In such cases, the order of the underlying differential operator effectively decreases by two in the singular limit as $\varepsilon \to 0$. In contrast, considerably fewer results are available for fourth-order problems of convection–diffusion type, such as (1), where the highest-order derivative decreases only by one. The available literature mainly addresses conforming finite element or finite difference methods. For example, Sun and Stynes studied a C^1-conforming finite element method for general even-order convection–diffusion problems in [10]. In [11, 12], the authors transformed a fourth-order convection–diffusion equation into a weakly coupled system of second-order equations and applied finite difference schemes combined with asymptotic expansion techniques.

More recently, WG-FEMs have emerged as an effective framework for the numerical approximation of higher-order differential equations [13]. By utilizing discontinuous polynomial spaces and weakly defined differential operators, the WG-FEM avoids the construction of globally C^1-conforming elements while retaining strong stability and flexibility on general meshes [14, 15]. The WG-FEM has been successfully applied to a variety of second- and higher-order singularly perturbed problems [16–18], including elliptic and parabolic equations. However, its application to singularly perturbed fourth-order convection–diffusion problems remains largely unexplored.

The main purpose of this paper is to develop and analyze a WG-FEM for the singularly perturbed fourth-order convection–diffusion Problem (1). It is worth emphasizing that uniform high-order convergence cannot be achieved on standard quasi-uniform meshes due to the explicit dependence of higher-order derivatives of the exact solution on ε^{-1}; see Lemma 2.1. In particular, the proposed method is developed for a fourth-order singularly perturbed convection–diffusion problem with mixed boundary

conditions, which has not been extensively addressed in the existing weak Galerkin literature. Moreover, the stabilization framework is specifically designed to accommodate this higher-order structure, and an ε-uniform error analysis is established on Shishkin meshes. These aspects clearly distinguish the present work from previous studies and clarify its original contribution.

Our analysis is based on the construction of suitable weak differential operators, including the weak first- and second-order derivatives and the weak convection operator, together with elementwise L^2-projection operators. A key ingredient in the proposed weak Galerkin framework is the appropriate choice of stabilization parameters, which guarantees stability and convergence uniformly with respect to the singular perturbation parameter. Although the analysis is carried out on a Shishkin mesh, the methodology and theoretical results can be extended in a straightforward manner to other layer-adapted meshes, such as Shishkin–Bakhvalov and Bakhvalov-type meshes.

The remainder of this paper is organized as follows. In Section 2, we present a decomposition of the exact solution and describe the construction of the Shishkin mesh. Section 3 is devoted to the formulation of the WG-FEM, where the weak first- and second-order derivatives and the weak convection operator are introduced. In Section 4, we define the local L^2-projection operators and establish their approximation properties. Section 5 is concerned with the stability and convergence analysis of the proposed WG-FEM, where parameter-uniform error estimates are derived in a suitable energy norm. Numerical experiments validating the theoretical results are reported in Section 6. Finally, concluding remarks and directions for future research are given in Section 7.

Throughout the remainder of the paper, the symbol C denotes a generic positive constant that is independent of ε and N, whose value may change from line to line. We also denote the derivatives of a function u as either u' or Du and u'' or D^2u, depending on which notation is more appropriate in the given context.

2. The solution decomposition and Shishkin mesh

2.1. Continuous problem

Let $(\cdot,\cdot)$ denote the $L^2(0,1)$ inner product and let $\|\cdot\|$ be the associated norm. For $m = 0, 1, 2$, we use $H^m(0,1)$ to denote the standard Sobolev space on $(0,1)$. We introduce the space

$$H_0^{1,2} = \{w \in H^2(0,1) \ : \ w(0) = w(1) = w'(0) = w''(1) = 0\}.$$

In our formulation, the continuous weak space $H_0^{1,2}$ is defined primarily for analysis and establishing consistency.

For $\phi, w \in H_0^{1,2}$, define the bilinear form

$$B_\varepsilon(\phi, w) = \varepsilon(\phi'', w'') + (\kappa\phi'', w') + (\eta\phi', w') + (\rho\phi' + \sigma\phi, w). \tag{3}$$

The corresponding energy norm is induced by

$$\|w\|_{CE}^2 := B_\varepsilon(w, w).$$

Using integration by parts and exploiting the boundary conditions $w(0) = w(1) = w'(0) = 0$, we obtain

$$B_\varepsilon(w, w) = \varepsilon(w'', w'') + (\kappa w'', w') + (\eta w', w') + (\rho w' + \sigma w, w)$$

$$
\begin{aligned}
&= \varepsilon \|w''\|^2 + (1, \tfrac{1}{2}(\kappa (w')^2)') + ((\eta - \tfrac{1}{2}\kappa')w', w') + (1, \tfrac{1}{2}(\rho w^2)') + ((\sigma - \tfrac{1}{2}\rho')w, w) \\
&= \varepsilon \|w''\|^2 + \tfrac{1}{2}\kappa(1)(w'(1))^2 + \left\|(\eta - \tfrac{1}{2}\kappa')^{1/2} w'\right\|^2 + \left\|(\sigma - \tfrac{1}{2}\rho')^{1/2} w\right\|^2 \\
&= \varepsilon \|w''\|^2 + ((\eta - \tfrac{1}{2}\kappa')w', w') + ((\sigma - \tfrac{1}{2}\rho')w, w) + \tfrac{1}{2}\kappa(1)(w'(1))^2.
\end{aligned}
$$

Hence, the energy norm can be written as

$$
\|w\|_{CE}^2 = \varepsilon \|w''\|^2 + \|(\eta - \tfrac{1}{2}\kappa')^{1/2} w'\|^2 + \|(\sigma - \tfrac{1}{2}\rho')^{1/2} w\|^2 + \tfrac{1}{2}\kappa(1)(w'(1))^2. \tag{4}
$$

Note that this property justifies the choice of the boundary condition $v'(0) = 0$ rather than imposing $v'(1) = 0$.

The weak formulation of Problem (1) is as follows: Find $v \in H_0^{1,2}$ such that

$$
B_\varepsilon(v, w) = (h, w), \qquad \forall\, w \in H_0^{1,2}. \tag{5}
$$

Standard arguments based on the Lax–Milgram lemma, together with those in [10, Lemma 2.1], show that the variational Problem (5) admits a unique solution in $H_0^{1,2}$.

For the subsequent error analysis, it is necessary to establish suitable regularity properties of the exact solution.

Lemma 2.1 (Solution decomposition and layer bounds)**.** *Let $q \in \mathbb{N}_0$ be fixed. Assume that the coefficients of Problem* (1) *are sufficiently smooth and satisfy the structural condition* (2)*. Then the solution v of Problem* (1) *admits the decomposition*

$$
v = v_r + v_\ell,
$$

where v_r is a regular component and v_ℓ is a boundary layer component associated with the endpoint $x = 1$. Moreover, a constant $C > 0$ exist independent of the perturbation parameter ε, such that the following estimates hold:

$$
\begin{aligned}
&\left|v_r^{(j)}(x)\right| \le C, && x \in [0, 1], \\
&\left|v_\ell^{(j)}(x)\right| \le C\, \varepsilon^{2-j} \exp\left(-\frac{\kappa_0(1 - x)}{\varepsilon}\right), && x \in [0, 1],
\end{aligned} \tag{6}
$$

for all integers $j = 0, 1, \ldots, q$.

Proof. A refined asymptotic representation of the solution can be obtained from classical singular perturbation theory. Following [19, Theorem 1.4] with $m = 4$, we infer that the solution v admits the expansion

$$
v(x) = H(x, \varepsilon) + \varepsilon^2 H_1(x, \varepsilon) \exp\left(-\frac{1}{\varepsilon}\int_x^1 \kappa(t)\, dt\right), \tag{7}
$$

where the functions H and H_1 are sufficiently smooth. Moreover, for any fixed integer $q \ge 0$, their derivatives satisfy the uniform bounds

$$
\left|H^{(j)}(x, \varepsilon)\right| + \left|H_1^{(j)}(x, \varepsilon)\right| \le C, \qquad x \in [0, 1], \quad j = 0, 1, \ldots, q,
$$

with a constant $C > 0$ that is independent of ε.

Combining the asymptotic representation (7) with arguments analogous to those in [3, Theorem 2.46], the solution v of Problem (1) can be decomposed as

$$v = v_r + v_\ell,$$

where v_r denotes the regular component and v_ℓ represents the boundary layer component. The estimates in (6) follow directly from this representation, which completes the proof. □

To construct a robust numerical scheme for Problem (1), we use a layer-adapted piecewise uniform mesh of Shishkin type, designed to accurately capture the boundary layer near the right endpoint $x = 1$ of the interval $[0, 1]$.

Let $N \geq 2$ be an even integer denoting the total number of subintervals. We introduce a mesh transition parameter $\lambda \in (0, 1/2]$, which separates the coarse region from the layer region and define it as

$$\lambda = \min\left\{\frac{1}{2},\ \frac{(r+1)\varepsilon}{\kappa_0}\ln N\right\}, \tag{8}$$

where r denotes the polynomial degree of the finite element approximation space, and κ_0 is given by (2). We assume that the perturbation parameter ε is sufficiently small relative to N so that

$$\frac{(r+1)\varepsilon}{\kappa_0}\ln N \leq \frac{1}{2},$$

which corresponds to the genuinely singularly perturbed regime. Under this assumption, the transition parameter simplifies to

$$\lambda = \frac{(r+1)\varepsilon}{\kappa_0}\ln N. \tag{9}$$

The computational domain $\Omega = (0, 1)$ is decomposed into two subregions

$$\Omega = \Omega_c \cup \Omega_f, \qquad \Omega_c = (0, 1-\lambda), \quad \Omega_f = (1-\lambda, 1).$$

Each of the subdomains Ω_c and Ω_f is partitioned uniformly into $N/2$ subintervals. The resulting mesh points $\{t_j\}_{j=0}^N$ are defined by

$$t_j = \begin{cases} \dfrac{2(1-\lambda)}{N}\, j, & j = 0, 1, \ldots, \dfrac{N}{2}, \\ 1 - \dfrac{2\lambda}{N}\Big(N - j\Big), & j = \dfrac{N}{2}+1, \ldots, N. \end{cases}$$

Let $\Omega = (0, 1)$ be subdivided into N nonoverlapping open subintervals by a strictly increasing sequence of nodes

$$0 = t_0 < t_1 < \cdots < t_N = 1,$$

where $N \in \mathbb{N}$ denotes the total number of elements. We denote this partition by

$$\mathcal{T}_N := \{I_j\}_{j=1}^N, \qquad I_j := (t_{j-1}, t_j).$$

For each element $I_j \in \mathcal{T}_N$, the local mesh width is defined as

$$k_j := t_j - t_{j-1} = \begin{cases} k_c, & j = 1, 2, \ldots, \dfrac{N}{2}, \\ k_f, & j = \dfrac{N}{2} + 1, \ldots, N, \end{cases}$$

where $k_c = \dfrac{2(1-\lambda)}{N}$ and $k_f = \dfrac{2\lambda}{N}$. One can then prove that

$$k_c = O(N^{-1}), \qquad k_f = O(\varepsilon N^{-1} \ln N). \tag{10}$$

This mesh construction provides a fine discretization in the layer region Ω_f while retaining a coarse, computationally efficient mesh in the regular region Ω_c.

3. The WG-FEM method

For each interval $I_j = (t_{j-1}, t_j)$, a weak function is defined as $w_j = \{w_j^{\mathrm{o}}, w_j^{\partial}, w_j^{g}\}$, where the interior component satisfies $w_j^{\mathrm{o}} \in L^2(I_j)$, and the boundary components satisfy $w_j^{\partial}, w_j^{g} \in L^{\infty}(\partial I_j)$. Here, w_j^{∂} and w_j^{g} represent independent boundary degrees of freedom approximating the trace of w_j^{o} and its derivative on ∂I_j, respectively.

Accordingly, the local weak Galerkin space on I_j is defined as

$$W(I_j) = \{w_j^{\mathrm{o}}, w_j^{\partial}, w_j^{g}\} : w_j^{\mathrm{o}} \in L^2(I_j),\ w_j^{\partial}, w_j^{g} \in L^{\infty}(\partial I_j)\}. \tag{11}$$

The Sobolev space $H^2(I_j)$ can be embedded in the space $W(I_j)$ by a map $\mathcal{W}_W : H^2(I_j) \to W(I_j)$ defined by $\mathcal{W}_W(\Phi) = \{\Phi|_{L^2(I_j)}, \Phi|_{\partial I_j}, \Phi'|_{\partial I_j}\}$ for $\Phi \in H^2(I_j)$. This implies that the Sobolev space $H^2(I_j)$ can be considered as a subspace of $W(I_j)$.

The discrete weak function space $\mathcal{W}_N(I_j)$ is defined as

$$\mathcal{W}_N(I_j) = \{w = \{w^{\mathrm{o}}, w^{\partial}, w^{g}\} : w^{\mathrm{o}} \in \mathbb{P}_r(I_j),\ w^{\partial}, w^{g} \in \mathbb{P}_0(\partial I_j)\}, \tag{12}$$

where $\mathbb{P}_r(I_j)$ denotes the space of polynomials in I_j of a degree of at most $r \geq 2$, and $\mathbb{P}_0(\partial I_j)$ is the space of constant polynomials on ∂I_j.

The global weak Galerkin space $\mathcal{W}_N$ is obtained by assembling the local spaces $\mathcal{W}_N(I_j)$ and identifying the boundary degrees of freedom at the mesh points. Specifically, for any $w = \{w^{\mathrm{o}}, w^{\partial}, w^{g}\} \in \mathcal{W}_N$ with $w|_{I_j} = w_j$, we require

$$w_j^{\partial}(t_j) = w_{j+1}^{\partial}(t_j), \qquad w_j^{g}(t_j) = w_{j+1}^{g}(t_j), \qquad j = 1, 2, \ldots, N-1.$$

Equivalently, the global weak Galerkin space can be written as follows, for $j = 1, \ldots, N-1$:

$$\mathcal{W}_N = \left\{w = \{w^{\mathrm{o}}, w^{\partial}, w^{g}\} \ :\ w|_{I_j} \in \mathcal{W}_N(I_j),\ w_j^{\partial}(t_j) = w_{j+1}^{\partial}(t_j),\ w_j^{g}(t_j) = w_{j+1}^{g}(t_j)\right\}.$$

We also define $\mathcal{W}_N^{\mathrm{o}}$ as the subspace of $\mathcal{W}_N$ as

$$\mathcal{W}_N^{\mathrm{o}} = \{w = \{w^{\mathrm{o}}, w^{\partial}, w^{g}\} \in \mathcal{W}_N :\ w^{\partial}(0) = w^{\partial}(1) = w^{g}(0) = 0\}.$$

To approximate Problem (1a),(1b), we use a weak Galerkin finite element space consisting of functions of the form $w = \{w^{\mathrm{o}}, w^{\partial}, w^{g}\}$, where w^{o} denotes the interior value on each element, w^{∂} represents the approximation of the trace of w on element boundaries, and w^{g} approximates the first derivative on the boundary.

The boundary conditions are incorporated in a manner consistent with the structure of the weak Galerkin method. The Dirichlet conditions $v(0) = \gamma_0$ and $v(1) = \gamma_1$ are imposed strongly by prescribing $w^{\partial}(0) = \gamma_0,$ and $w^{\partial}(1) = \gamma_1$. Similarly, the first-derivative boundary condition $v'(0) = \zeta_0$ is enforced by setting the boundary value of the discrete weak derivative, $w^{g}(0) = \zeta_0$.

In contrast, the second-derivative boundary condition $v''(1) = \zeta_1$ is not imposed strongly, as the weak Galerkin space does not include an explicit degree of freedom associated with second derivatives. Instead, this condition is treated as a natural boundary condition and is incorporated into the formulation through the boundary terms arising from the variational formulation. Specifically, following integration by parts, boundary contributions involving $v''(1)$ appear in the weak form and are replaced by the prescribed data ζ_1. At the discrete level, this condition is enforced weakly through the discrete weak derivatives in conjunction with appropriate boundary stabilization terms, thereby ensuring consistency with the continuous problem.

This approach enables the method to accommodate boundary conditions of different orders within a unified variational framework while maintaining both flexibility and consistency.

We now define the weak derivatives of a weak function $w = \{w^{\mathrm{o}}, w^{\partial}, w^{g}\} \in \mathcal{W}_N$.

The weak second-order derivative $D^2_{w,r-2}w \in \mathbb{P}_{r-2}(I_j)$ is defined by

$$(D^2_{w,r-2}w, \Phi)_{L^2(I_j)} = (w^{\mathrm{o}}, \Phi'')_{L^2(I_j)} - \langle w^{\partial}, \Phi'\mathbf{n}\rangle_{\partial I_j} + \langle w^{g}\mathbf{n}, \Phi\rangle_{\partial I_j}, \quad \forall\, \Phi \in \mathbb{P}_{r-2}(I_j). \tag{13}$$

Similarly, the weak first derivative $D_{w,r-1}w \in \mathbb{P}_{r-1}(I_j)$ is defined by

$$(D_{w,r-1}w, \Phi)_{L^2(I_j)} = -(w^{\mathrm{o}}, \Phi')_{L^2(I_j)} + \langle w^{\partial}, \Phi\mathbf{n}\rangle_{\partial I_j}, \quad \forall\, \Phi \in \mathbb{P}_{r-1}(I_j). \tag{14}$$

Here, $(\cdot,\cdot)_{L^2(I_j)}$ denotes the standard inner product on $L^2(I_j)$, and the boundary pairing is defined by

$$\langle v, z\mathbf{n}\rangle_{\partial I_j} := v(t_j)z(t_j) - v(t_{j-1})z(t_{j-1}),$$

where $\mathbf{n}$ denotes the outward unit normal on ∂I_j.

The weak convection derivative $D^{\rho}_{w,r}w \in \mathbb{P}_r(I_j)$ of w is defined by

$$(D^{\rho}_{w,r}w, \Phi)_{L^2(I_j)} = -(w^{\mathrm{o}}, (\rho\Phi)')_{L^2(I_j)} + \langle w^{\partial}, \rho\Phi\mathbf{n}\rangle_{\partial I_j}, \quad \forall \Phi \in \mathbb{P}_r(I_j). \tag{15}$$

For $r \geq 2$, the discrete weak derivatives $D^2_{w,r-2}$, $D_{w,r-1}$, and $D^{\rho}_{w,r}$ are computed on $\mathcal{W}_N$ by (13)–(15) on each interval I_j, respectively. That is, for $\phi \in \mathcal{W}_N$, we have

$$(D^2_{w,r-2}\phi)|_{I_j} = D^2_{w,r-2}(\phi|_{I_j}),\ (D_{w,r-1}\phi)|_{I_j} = D_{w,r-1}(\phi|_{I_j}),\ (D^{\rho}_{w,r}\phi)|_{I_j} = D^{\rho}_{w,r}(\phi|_{I_j}).$$

Since the polynomial degrees $r-2$, $r-1$, and r are fixed throughout the analysis, we henceforth drop the subscripts and simply write D^2_w, D_w, and D^{ρ}_w for notational convenience.

We introduce the following bilinear forms:

$$(D^2_w\psi, D^2_w\phi) := \sum_{j=1}^{N}(D^2_w\psi, D^2_w\phi)_{L^2(I_j)}, \quad (D_w\psi, D_w\phi) := \sum_{j=1}^{N}(D_w\psi, D_w\phi)_{L^2(I_j)},$$

$$(D_w^2\psi, D_w\phi) := \sum_{j=1}^{N}(D_w^2\psi, D_w\phi)_{L^2(I_j)},$$

$$s_d(\psi,\phi) := \sum_{j=1}^{N}\Big(\theta_j\langle(\psi^{\rm o})' - \psi^g,\, D\phi^{\rm o} - \phi^g\rangle_{\partial I_j} + \mu_j\langle\psi^{\rm o} - \psi^\partial,\, \phi^{\rm o} - \phi^\partial\rangle_{\partial I_j}\Big),$$

$$s_c(\psi,\phi) := \sum_{j=1}^{N}\langle\rho\,\mathbf{n}\,(\psi^{\rm o} - \psi^\partial),\, \phi^{\rm o} - \phi^\partial\rangle_{\partial_+ I_j}, \quad (\psi^{\rm o},\phi^{\rm o}) := \sum_{j=1}^{N}(\psi^{\rm o},\phi^{\rm o})_{L^2(I_j)}.$$

Here, the inflow boundary is defined by

$$\partial_+ I_j := \{\, t \in \partial I_j : \rho(t)\mathbf{n}(t) \geq 0 \,\}.$$

The stabilization parameters μ_j and θ_j are given by

$$\mu_j = \begin{cases} N, & j = 1,\ldots,\frac{N}{2}, \\ N(\ln N)^{-1}, & j = \frac{N}{2}+1,\ldots,N, \end{cases} \tag{16}$$

and

$$\theta_j = \begin{cases} 1, & j = 1,\ldots,\frac{N}{2}, \\ \dfrac{N}{\ln N}, & j = \frac{N}{2}+1,\ldots,N. \end{cases} \tag{17}$$

Remark 3.1. These parameters are chosen in such a way that a parameter-robust convergence can be established. The stabilization parameters in the fourth-order problems are usually taken as

$$\mu_j = \varepsilon k_j^{-3} + k_j^{-1} \quad \text{and} \quad \theta_j = \varepsilon k_j^{-1}.$$

However, with these choices we are unable to derive the ε-uniform error estimates required in our analysis.

We now present the proposed numerical scheme. The weak Galerkin finite element approximation of (1) seeks $v_N = \{v^{\rm o}, v^\partial, v^g\} \in \mathcal{W}_N$ such that the boundary data are incorporated as

$$v^\partial(0) = \gamma_0, \quad v^\partial(1) = \gamma_1, \quad v^g(0) = \zeta_0,$$

and the following discrete weak formulation holds:

$$\mathcal{B}(v_N,\phi_N) = L(h,\phi_N) := (h,\phi^{\rm o}) + \varepsilon\zeta_1\phi^g(1), \qquad \forall\, \phi_N = \{\phi^{\rm o},\phi^\partial,\phi^g\} \in \mathcal{W}_N^{\rm o}, \tag{18}$$

where the bilinear form $\mathcal{B}(\cdot,\cdot)$ is defined by

$$\mathcal{B}(v_N,\phi_N) := B_D(v_N,\phi_N) + B_d(v_N,\phi_N) + S(v_N,\phi_N),$$

with

$$B_D(v_N,\phi_N) = \varepsilon\,(D_w^2 v_N, D_w^2\phi_N) + \frac{1}{2}\Big((\kappa D_w^2 v_N, D_w\phi_N) - (\kappa D_w v_N, D_w^2\phi_N)\Big),$$

$$+\frac{1}{2}\kappa(1)v^g(1)\phi^g(1), \tag{19}$$

$$B_d(v_N,\phi_N) = (\eta D_w v_N, D_w\phi_N) + (\rho D_w^o v_N + \sigma v^o, \phi^o),$$

$$S(v_N,\phi_N) = s_d(v_N,\phi_N) + s_c(v_N,\phi_N).$$

In this formulation, the discrete weak derivatives D_w and D_w^2 are used to approximate first- and second-order derivatives, respectively, while the stabilization terms s_d and s_c ensure the stability and consistency of the method. The incorporation of the boundary values v^∂ and v^g allows the exact enforcement of the nonhomogeneous boundary conditions in the discrete scheme.

We note that the additional term $v^g(1)\,\phi^g(1)$ in (19) arises naturally from the treatment of the third-order derivative via integration by parts. In particular, for the terms $-(\kappa v'')'$ and $\varepsilon v^{(4)}$ in the differential operator, integration by parts over Ω gives, respectively

$$\int_0^1 -(\kappa v'')'\, w\, dx = \frac{1}{2}\Big((\kappa v'', w') - (\kappa v', w'')\Big) - \frac{1}{2}(\kappa' v', w') + \frac{1}{2}\,\kappa(1)\,v'(1)\,w'(1).$$

and

$$\int_\Omega \varepsilon v^{(4)}\, w\, dx = \varepsilon \int_\Omega v''\, w''\, dx + \varepsilon\Big[v'''\, w - v''\, w'\Big]_0^1 = \varepsilon \int_\Omega v''\, w''\, dx - \varepsilon v''(1)w'(1),$$

if a function w satisfies $w(0) = w(1) = w'(0) = 0$. In the weak Galerkin framework, boundary contributions are incorporated through the discrete boundary unknowns w^∂ and w^g, where w^g serves as an approximation to the trace of the derivative w' on the boundary. Consequently, the first-derivative boundary condition at $x = 1$ is weakly enforced via the term

$$v^g(1)\, w^g(1),$$

which appears in the bilinear form $B_D(v_N, w_N)$ defined in (19).

Furthermore, the second-derivative boundary condition at $x = 1$ is imposed through the consistency term

$$v''(1)\, w^g(1) = \zeta_1\, w^g(1),$$

which is incorporated into the linear functional $L(h, w_N)$ in (18).

These constructions ensure that the nonhomogeneous boundary data, together with the higher-order condition $v''(1) = \zeta_1$, are accurately represented at the discrete level, while preserving consistency with the underlying continuous formulation.

Let $\phi = \{\phi^o, \phi^\partial, \phi^g\} \in \mathcal{W}_N$. An energy norm $\|\cdot\|_E$ in $\mathcal{W}_N$ is defined by

$$\|\phi\|_E^2 := \varepsilon\|D_w^2\phi\|^2 + \eta_0\|D_w\phi\|^2 + \rho_0\|\phi^o\|^2 + |\phi|_\rho^2 + \frac{1}{2}\kappa(1)(\phi^g)^2(1) + s_d(\phi,\phi), \tag{20}$$

where $|\phi|_\rho^2 := \sum_{j=1}^N c_j|\sqrt{|\rho|}(\phi^o - \phi^\partial)|^2(t_j^-)$ with

$$c_j = \begin{cases} \frac{1}{2}, & j = N, \\ 1, & j = 1,\ldots,N-1. \end{cases}$$

An energy norm $\|\cdot\|_{\mathcal{D}}^2$ on $\mathcal{W}_N + H_0^1(\Omega)$, incorporating the classical derivatives, is defined by

$$\|\phi\|_{\mathcal{D}}^2 := \varepsilon\|D^2\phi^{\mathrm{o}}\|^2 + \eta_0\|D\phi^{\mathrm{o}}\|^2 + \rho_0\|\phi^{\mathrm{o}}\|^2 + |\phi|_\rho^2 + \frac{1}{2}\kappa(1)(\phi^g)^2(1) + s_d(\phi,\phi), \tag{21}$$

where D^2v and Dv are the second and first derivatives of a function v, respectively.

To show that $\|\phi\|_E$ defines a norm, it suffices to verify its definiteness, since the positivity and the triangle inequality follow directly from the structure of the terms and the standard properties of L^2-based norms. A similar argument applies to $\|\phi\|_{\mathcal{D}}$.

Assume that $\|\phi\|_E = 0$. Then each non-negative term in the definition of $\|\cdot\|_E$ must vanish, yielding

$$D_w^2\phi = 0, \quad D_w\phi = 0, \quad \phi^{\mathrm{o}} = 0 \quad \text{in } \Omega,$$

together with

$$|\phi|_\rho = 0, \qquad s_d(\phi,\phi) = 0, \qquad \phi^g(1) = 0.$$

Since $\phi^{\mathrm{o}} = 0$, the weak derivative identity for $D_w\phi = 0$ implies

$$\langle\phi^\partial, v\rangle_{\partial I_j} = 0 \quad \forall v \in P_r(I_j),$$

which yields $\phi^\partial = 0$ on each element boundary. Similarly, $D_w^2\phi = 0$ together with $\phi^{\mathrm{o}} = 0$ enforces $\phi^g = 0$ through the corresponding weak consistency relations.

Moreover, $|\phi|_\rho = 0$ guarantees continuity of traces at interior nodes, while $s_d(\phi,\phi) = 0$ enforces consistency between the interior and boundary components.

Consequently,

$$\phi^{\mathrm{o}} = 0, \quad \phi^\partial = 0, \quad \phi^g = 0,$$

and hence $\phi = 0$ in $\mathcal{W}_N + H_0^1(\Omega)$.

Therefore, $\|\cdot\|_E$ is definite, and thus is a norm. The same conclusion holds for $\|\cdot\|_{\mathcal{D}}$.

Lemma 3.2 (One-dimensional interior and edge duality estimates)**.** *Let $I = (t_{j-1}, t_j) \in \mathcal{T}_h$ with $k_j = t_j - t_{j-1}$ and let $h = \max_{j=1,\dots,N} k_j$. For a weak Galerkin function $w = \{w^{\mathrm{o}}, w^\partial, w^g\}$ on I and its weak derivative $D_w w$, the following estimates hold:*

$$\|(w^{\mathrm{o}})'\|_{L^2(I)} \le \|D_w w\|_{L^2(I)},$$

and for each endpoint $t_e \in \{t_{j-1}, t_j\}$,

$$|w^{\mathrm{o}}(t_e) - w^\partial(t_e)| \le Ch^{1/2}\|D_w w\|_{L^2(I)},$$

where $C > 0$ is independent of h.

Proof. Assume $w^{\mathrm{o}} \in \mathbb{P}_r(I)$. Define

$$D(r, I) := \{q \in \mathbb{P}_r(I) : q(t_{j-1}) = q(t_j) = 0\}.$$

Since differentiation maps $\mathbb{P}_r(I)$ onto $\mathbb{P}_{r-1}(I)$ and

$$\dim D(r, I) = \dim \mathbb{P}_{r-1}(I),$$

the space $D(r, I)$ provides a dual test space for $\mathbb{P}_{r-1}(I)$. Hence, for any we have $w \in \mathbb{P}_{r-1}(I)$,

$$\|w\|_{L^2(I)} = \sup_{q \in D(r,I)} \frac{(w, q)_I}{\|q\|_{L^2(I)}}.$$

Taking $w = (w^{\mathrm{o}})' \in \mathbb{P}_{r-1}(I)$, we have

$$\|(w^{\mathrm{o}})'\|_{L^2(I)} = \sup_{q \in D(r,I)} \frac{((w^{\mathrm{o}})', q)_I}{\|q\|_{L^2(I)}}.$$

For $q \in D(r, I)$, the boundary term in the definition of $D_w w$ vanishes. Integration by parts yields

$$((w^{\mathrm{o}})', q)_I = (D_w w, q)_I.$$

Therefore,

$$\|(w^{\mathrm{o}})'\|_{L^2(I)} = \sup_{q \in D(r,I)} \frac{(D_w w, q)_I}{\|q\|_{L^2(I)}} \leq \|D_w w\|_{L^2(I)},$$

by the Cauchy–Schwarz inequality.

Let t_e be one endpoint of I and define

$$D_e(r, I) := \{q \in \mathbb{P}_r(I) : q = 0 \text{ at the endpoint of } I \text{ different from } t_e\}.$$

Since evaluation at a point is a linear functional, we have

$$|w^{\mathrm{o}}(t_e) - w^{\partial}(t_e)| = \sup_{q \in D_e(r,I)} \frac{\langle w^{\mathrm{o}} - w^{\partial}, qn \rangle_e}{|q(t_e)|}.$$

For $q \in D_e(r, I)$, integration by parts gives

$$(D_w w, q)_I = ((w^{\mathrm{o}})', q)_I + \langle w^{\partial} - w^{\mathrm{o}}, qn \rangle_e.$$

Choosing $q \in D_e(r, I)$ such that $((w^{\mathrm{o}})', q)_I = 0$, we obtain

$$\langle w^{\partial} - w^{\mathrm{o}}, qn \rangle_e = (D_w w, q)_I.$$

Hence

$$|\langle w^{\partial} - w^{\mathrm{o}}, qn \rangle_e| \leq \|D_w w\|_{L^2(I)} \|q\|_{L^2(I)}.$$

By the one-dimensional inverse trace inequality for polynomial spaces, we have

$$\|q\|_{L^2(I)} \leq C h^{1/2} |q(t_e)|.$$

Therefore

$$|w^{\mathrm{o}}(t_e) - w^{\partial}(t_e)| \leq C h^{1/2} \|D_w w\|_{L^2(I)}.$$

This completes the proof. □

We show that these two norms defined by (20) and (21) are comparable in $\mathcal{W}_N^{\mathrm{o}}$.

Lemma 3.3. *Let $\phi = \{\phi^{\mathrm{o}}, \phi^{\partial}, \phi^{g}\} \in \mathcal{W}_N^{\mathrm{o}}$. One then has the following inequalities:*

$$\|\phi\|_{\mathcal{D}} \leq C\|\phi\|_E.$$

Proof. To obtain the lower bound, we take $\Phi = D^2\phi^{\mathrm{o}}$ in the definition of the discrete weak second derivative (13) to obtain

$$\begin{aligned}(D_w^2\phi, D^2\phi^{\mathrm{o}})_{L^2(I_j)} = (D^2\phi^{\mathrm{o}}, D^2\phi^{\mathrm{o}})_{L^2(I_j)} + \langle \phi^{\mathrm{o}} - \phi^{\partial}, (D^2\phi^{\mathrm{o}})'\mathbf{n}\rangle_{\partial I_j} \\ + \langle \phi^{g} - D\phi^{\mathrm{o}}, D^2\phi^{\mathrm{o}}\mathbf{n}\rangle_{\partial I_j}.\end{aligned}$$

Applying the Cauchy–Schwarz inequality together with the trace inequality yields

$$\begin{aligned}\|D^2\phi^{\mathrm{o}}\|_{L^2(I_j)}^2 &\leq \|D^2\phi^{\mathrm{o}}\|_{L^2(I_j)}\|D_w^2\phi\|_{L^2(I_j)} + \|\phi^{\mathrm{o}} - \phi^{\partial}\|_{L^2(\partial I_j)}\|(D^2\phi^{\mathrm{o}})'\|_{L^2(\partial I_j)} \\ &\quad + \|\phi^{g} - D\phi^{\mathrm{o}}\|_{L^2(\partial I_j)}\|D^2\phi^{\mathrm{o}}\|_{L^2(\partial I_j)} \\ &\leq C\Big(\|D_w^2\phi\|_{L^2(I_j)} + k_j^{-3/2}\|\phi^{\mathrm{o}} - \phi^{\partial}\|_{L^2(\partial I_j)} \\ &\quad + k_j^{-1/2}\|\phi^{g} - D\phi^{\mathrm{o}}\|_{L^2(\partial I_j)}\Big)\|D^2\phi^{\mathrm{o}}\|_{L^2(I_j)}.\end{aligned}$$

Hence,

$$\begin{aligned}\varepsilon\|D^2\phi^{\mathrm{o}}\| &\leq C\Big(\varepsilon\|D_w^2\phi\| + \sum_{j=1}^{N}(\varepsilon k_j^{-3}\|\phi^{\mathrm{o}} - \phi^{\partial}\|_{L^2(\partial I_j)} \\ &\quad + \varepsilon k_j^{-1}\|\phi^{g} - D\phi^{\mathrm{o}}\|_{L^2(\partial I_j)})\Big) \\ &\leq C\Big(\varepsilon\|D_w^2\phi\| + s_d(\phi,\phi)\Big).\end{aligned}$$

From Lemma 3.2, we also have

$$\begin{aligned}\|D\phi^{\mathrm{o}}\|^2 &\leq C\Big(\|D_w\phi\|^2 + \sum_{j=1}^{N} k_j^{-1}\|\phi^{\mathrm{o}} - \phi^{\partial}\|_{L^2(\partial I_j)}^2\Big) \\ &\leq C\|D_w\phi\|^2.\end{aligned}$$

Recalling the definitions of the two norms, we conclude that

$$\|\phi\|_{\mathcal{D}} \leq C\|\phi\|_E,$$

which completes the proof. □

We shall prove that the bilinear form $\mathcal{B}(\cdot,\cdot)$ is coercive with respect to the energy norm $\|\cdot\|_E$ defined in (20).

Lemma 3.4. *The bilinear form $\mathcal{B}(\cdot,\cdot)$ is coercive with respect to the energy norm $\|\cdot\|_E$, i.e.,*

$$\mathcal{B}(\phi,\phi) \geq \|\phi\|_E^2, \qquad \forall\, \phi \in \mathcal{W}_N^{\mathrm{o}}. \tag{22}$$

Proof. From the definition of the bilinear form $\mathcal{B}(\cdot,\cdot)$, it follows that for any $\phi \in \mathcal{W}_N^{\mathrm{o}}$, we have

$$\mathcal{B}(\phi,\phi) \geq \varepsilon\|D_w^2\phi\|^2 + \eta_0\|D_w\phi\|^2 + \rho_0\|\phi^{\mathrm{o}}\|^2 + (D_w^{\rho}\phi,\phi^{\mathrm{o}}) + \frac{1}{2}\kappa(1)(\phi^g)^2(1) + S(\phi,\phi).$$

Applying Inequality (3.12) from [20], we have

$$\|\phi^{\mathrm{o}}\|^2 + (D_w^{\rho}\phi,\phi^{\mathrm{o}}) + s_c(\phi,\phi) \geq \|\sqrt{\rho_0}\,\phi^{\mathrm{o}}\|^2 + |\phi|_{\rho}^2.$$

Combining the two inequalities above yields

$$\mathcal{B}(\phi,\phi) \geq \varepsilon\|D_w^2\phi\|^2 + \eta_0\|D_w\phi\|^2 + \rho_0\|\phi^{\mathrm{o}}\|^2 + |\phi|_{\rho}^2 + \frac{1}{2}\kappa(1)(\phi^g)^2(1) + S(\phi,\phi) = \|\phi\|_E^2.$$

This completes the proof. □

Combining Lemma 3.3 with Lemma 3.4, we conclude that the bilinear form $\mathcal{B}(\cdot,\cdot)$ is coercive on $\mathcal{W}_N^{\mathrm{o}}$ with respect to the norm $\|\cdot\|_{\mathcal{D}}$. More precisely, there is a positive constant C, independent of the discretization parameters, such that

$$\mathcal{B}(\phi,\phi) \geq C\|\phi\|_{\mathcal{D}}^2, \qquad \forall\, \phi \in \mathcal{W}_N^{\mathrm{o}}. \tag{23}$$

4. Projection operator

This section is devoted to the construction of suitable projection operators associated with the weak Galerkin finite element space and to the derivation of their basic approximation properties.

Let $r \geq 0$ be a fixed integer. For each element $I_j = (t_{j-1}, t_j)$, $j = 1, 2, \ldots, N$, we define the elementwise L^2–projection $\mathcal{P}_j^r : L^2(I_j) \to \mathbb{P}_r(I_j)$ by the relation

$$(\mathcal{P}_j^r w - w, q)_{L^2(I_j)} = 0, \qquad \forall\, q \in \mathbb{P}_r(I_j).$$

For simplicity of notation, we write $\mathcal{P}_j^r w = \mathcal{P}_N^r w$ on I_j.

Next, we introduce a global projection operator $\mathcal{J} : H^2(\Omega) \to \mathcal{W}_N$ defined locally on each element I_j, $\quad j = 1, 2, \ldots, N$ by

$$\mathcal{J}w\big|_{\tilde{I}_j} = \left\{\mathcal{J}^0 w, \mathcal{J}^{\partial} w, \mathcal{J}^g w\right\} = \left\{\mathcal{P}_N^r w,\ (w(t_{j-1}), w(t_j)),\ (w'(t_{j-1}), w'(t_j))\right\}. \tag{24}$$

By construction, if $w \in H_0^{1,2}(\Omega)$, then $\mathcal{J}w \in \mathcal{W}_N^{\mathrm{o}}$.

The projection $\mathcal{J}$ imposes a local stability property on each mesh element. There is a constant $C > 0$, independent of the mesh size, such that

$$\|\mathcal{J}^0 w\|_{L^2(I_j)} \leq C\,\|w\|_{L^2(I_j)}, \qquad j = 1, 2, \ldots, N. \tag{25}$$

This stability estimate plays a crucial role in the subsequent error analysis. In the following subsection, we derive approximation bounds for the projection $\mathcal{J}$ in both the L^2–norm and the weak energy norm.

The commutativity property of the projection operator $\mathcal{J}$ plays a central role in the error analysis of the WG-FEM.

Lemma 4.1 (Commutativity property)**.** *Let $w \in H_0^2(\Omega)$. Then, for each element I_j, the following identities hold:*

$$D_w(\mathcal{J}w) = \mathcal{J}^{\mathrm{o}}(Dw), \tag{26}$$

$$D_w^2(\mathcal{J}w) = \mathcal{J}^{\mathrm{o}}(D^2w). \tag{27}$$

Proof. We first prove (26). By the definition of the weak first derivative and integration by parts, for any $\phi \in \mathbb{P}_{r-1}(I_j)$ we obtain

$$(D_w(\mathcal{J}w), \phi)_{L^2(I_j)} = -(\mathcal{J}^{\mathrm{o}}w, \phi')_{L^2(I_j)} + (\mathcal{J}^{\partial}w, \phi\,\mathbf{n})_{\partial I_j}.$$

Using the definition of $\mathcal{J}$ and the fact that $\mathcal{J}^{\mathrm{o}}w$ is the L^2—projection of w, we have

$$-(\mathcal{J}^{\mathrm{o}}w, \phi')_{L^2(I_j)} + (\mathcal{J}^{\partial}w, \phi\,\mathbf{n})_{\partial I_j} = -(w, \phi')_{L^2(I_j)} + (w, \phi\,\mathbf{n})_{\partial I_j}.$$

Integration by parts then yields

$$-(w, \phi')_{L^2(I_j)} + (w, \phi\,\mathbf{n})_{\partial I_j} = (w', \phi)_{L^2(I_j)} = (\mathcal{J}^{\mathrm{o}}(Dw), \phi)_{L^2(I_j)},$$

which proves (26).

Next, we establish (27). From the definition of the weak second derivative, for any $\Phi \in \mathbb{P}_{r-2}(I_j)$, we have

$$(D_w^2(\mathcal{J}w), \Phi)_{L^2(I_j)} = (\mathcal{J}^{\mathrm{o}}w, \Phi'')_{L^2(I_j)} - (\mathcal{J}^{\partial}w, \Phi'\mathbf{n})_{\partial I_j} + (\mathcal{J}^{g}w\,\mathbf{n}, \Phi)_{\partial I_j}.$$

Invoking again the definition of $\mathcal{J}$ and integrating by parts twice, we obtain

$$\begin{aligned}(D_w^2(\mathcal{J}w), \Phi)_{L^2(I_j)} &= (w, \Phi'')_{L^2(I_j)} - (w, \Phi'\mathbf{n})_{\partial I_j} + (w'\mathbf{n}, \Phi)_{\partial I_j} \\ &= (w'', \Phi)_{L^2(I_j)} = (\mathcal{J}^{\mathrm{o}}(D^2w), \Phi)_{L^2(I_j)}.\end{aligned}$$

This completes the proof. □

We will repeatedly use the following inverse and trace inequalities (see [21]). For each element $I_j = (t_{j-1}, t_j)$ with a mesh size $k_j = t_j - t_{j-1}$, there is a constant $C > 0$, independent of k_j, such that

$$\begin{aligned}\|\Phi\|_{L^2(\partial I_j)}^2 &\le C\Big(k_j^{-1}\|\Phi\|_{L^2(I_j)}^2 + \|\Phi\|_{L^2(I_j)}\|\Phi'\|_{L^2(I_j)}\Big), && \forall\, \Phi \in H^1(I_j), \\ \|\Phi_N'\|_{L^2(I_j)} &\le Ck_j^{-1}\|\Phi_N\|_{L^2(I_j)}, && \forall\, \Phi_N \in \mathbb{P}_r(I_j), \\ \|\Phi_N\|_{L^2(\partial I_j)} &\le Ck_j^{-1/2}\|\Phi_N\|_{L^2(I_j)}, && \forall\, \Phi_N \in \mathbb{P}_r(I_j).\end{aligned} \tag{28}$$

Furthermore, standard projection theory yields the following local approximation estimates for the projection $\mathcal{J}^{\mathrm{o}}$:

$$\left\|(w - \mathcal{J}^{\mathrm{o}}w)^{(l)}\right\|_{L^s(I_j)} \le Ck_j^{r+1-l}\|w^{(r+1)}\|_{L^s(I_j)}, \qquad w \in W^{r+1,s}(I_j), \tag{29}$$

where $s \in \{2, \infty\}$ and $l = 0, 1$. The constant C is independent of k_j and w.

Lemma 4.2. *For an element $I_j = [t_{j-1}, t_j]$ and $w \in H^{r+1}(I_j)$, one has the following projection error estimates:*

$$\|(w - \mathcal{J}^{\mathrm{o}} w)^{(s)}\|_{L^2(\partial I_j)} \le C k_j^{r+1/2-s} |w|_{H^{r+1}(I_j)}. \tag{30}$$

Proof. The proof follows readily from the trace inequalities (28) together with the projection estimates (29). □

We next derive projection error bounds for the weak Galerkin projection on the Shishkin mesh. These estimates play a central role in the subsequent stability and convergence analysis. For $s = 0, 1, 2$, define the projection errors

$$\xi^{(s)}(u) := (u - \mathcal{J}^{\mathrm{o}} u)^{(s)}, \qquad \xi^s(u) := u^{(s)} - \mathcal{J}^{\mathrm{o}}(u^{(s)}), \tag{31}$$

for a function u, and adopt the convention $\xi = \xi^{(0)} = \xi^0$. Define the projection error functions associated with the regular and boundary layer components of the solution as

$$\xi_r^s := v_r^{(s)} - \mathcal{J}^{\mathrm{o}} v_r^{(s)}, \qquad \xi_\ell^s := v_\ell^{(s)} - \mathcal{J}^{\mathrm{o}} v_\ell^{(s)}.$$

Equivalently,

$$\xi_r^{(s)} := (v_r - \mathcal{J}^{\mathrm{o}} v_r)^{(s)}, \qquad \xi_\ell^{(s)} := (v_\ell - \mathcal{J}^{\mathrm{o}} v_\ell)^{(s)}, \qquad s = 0, 1, 2.$$

Lemma 4.3 (Projection error estimates on a Shishkin mesh)**.** *Let v be the solution of* (1) *and suppose that it admits the standard decomposition $v = v_r + v_\ell$, as described in Lemma 2.1. Let the mesh-dependent parameters μ_j and θ_j be defined as in* (16) *and* (17)*. Then there is a constant $C > 0$, independent of ε and N, such that the following estimates hold:*

$$\Big(\sum_{j=1}^{N} \|\xi^{(s)}\|_{L^2(I_j)}^2\Big)^{1/2} \le C\Big(\varepsilon^{(5-2s)/2}(N^{-1}\ln N)^{r+1-s} + N^{-(r+1-s)}\Big), \qquad s = 0, 1, 2, \tag{32}$$

$$\Big(\sum_{j=1}^{N} \frac{1}{\mu_j}\|\xi^2\|_{L^2(\partial I_j)}^2\Big)^{1/2} \le C(N^{-1}\ln N)^{(r-1)}, \tag{33}$$

$$\Big(\sum_{j=1}^{N} \frac{1}{\theta_j}\|\xi^1\|_{L^2(\partial I_j)}^2\Big)^{1/2} \le C N^{-r+1/2}, \tag{34}$$

$$\Big(\sum_{j=1}^{N} \frac{\varepsilon^2}{\theta_j}\|\xi^2\|_{L^2(\partial I_j)}^2\Big)^{1/2} \le C\,\varepsilon^{1/2}(N^{-1}\ln N)^{r-1}, \tag{35}$$

$$\Big(\sum_{j=1}^{N} \theta_j\|\xi^{(1)}\|_{L^2(\partial I_j)}^2\Big)^{1/2} \le C\,N^{-(r-1/2)}, \tag{36}$$

$$\Big(\sum_{j=1}^{N} \frac{\varepsilon^2}{\mu_j}\|(\xi_r^2)'\|_{L^2(\partial I_j)}^2\Big)^{1/2} \le C\,N^{-(r-1)}, \tag{37}$$

$$\sum_{j=\frac{N}{2}}^{N} \|(\xi_\ell^2)'\|_{L^\infty(I_j)} \le C\,\varepsilon^{-1}(N^{-1}\ln N)^{r-2}, \tag{38}$$

$$\Big(\sum_{j=1}^{N/2}\frac{\varepsilon^2}{\mu_j}\|(\xi_\ell^2)'\|^2_{L^2(\partial I_j)}\Big)^{1/2}\le C\,N^{-(r+1)}, \tag{39}$$

$$\Big(\sum_{j=1}^{N}\frac{1}{\mu_j}\|\xi^1\|^2_{L^2(\partial I_j)}\Big)^{1/2}\le CN^{-r}, \tag{40}$$

$$\Big(\sum_{j=1}^{N}\frac{1}{\mu_j}\|\xi\|^2_{L^2(\partial I_j)}\Big)^{\frac{1}{2}}\le CN^{-(r+1)}, \tag{41}$$

$$\Big(\sum_{j=1}^{N}\mu_j\|\xi\|^2_{L^2(\partial I_j)}\Big)^{1/2}\le CN^{-r}. \tag{42}$$

Proof. By the projection estimate (29) with $s=2$ and the regularity bounds (6), we obtain

$$\|\xi_r^{(s)}\|^2\le C\sum_{j=1}^{N}k_j^{2(r+1-s)}\|v_r^{(r+1)}\|^2_{L^2(I_j)}\le CN^{-2(r+1-s)}, \tag{43}$$

where we used $k_j\le CN^{-1}$ for all j.

For the layer component, the same arguments yield

$$\begin{aligned}\sum_{j=N/2+1}^{N}\|\xi_\ell^{(s)}\|^2_{L^2(I_j)}&\le C\sum_{j=\frac{N}{2}+1}^{N}k_j^{2(r+1-s)}\big\|v_\ell^{(r+1)}\big\|^2_{L^2(I_j)}\\&\le C\sum_{j=\frac{N}{2}+1}^{N}(\varepsilon N^{-1}\ln N)^{2(r+1-s)}\big\|\varepsilon^{1-r}e^{-\kappa_0(1-x)/\varepsilon}\big\|^2_{L^2(I_j)}\\&\le C\varepsilon^{4-2s}(N^{-1}\ln N)^{2(r+1-s)}\int_{1-\lambda}^{1}e^{-2\kappa_0(1-x)/\varepsilon}\,dx\\&\le C\varepsilon^{5-2s}(N^{-1}\ln N)^{2(r+1-s)}.\end{aligned} \tag{44}$$

With the aid of the stability estimate (25), an inverse inequality, and the estimate (6), we obtain

$$\begin{aligned}\sum_{j=1}^{N/2}\big\|\xi_\ell^{(s)}\big\|^2_{L^2(I_j)}&\le C\sum_{j=1}^{N/2}\Big(\big\|v_\ell^{(s)}\big\|^2_{L^2(I_j)}+k_j^{-2s}\big\|\mathcal{J}^{\mathrm{o}}v_\ell\big\|^2_{L^2(I_j)}\Big)\\&\le C\,\varepsilon^{2(2-s)}(1+\varepsilon^4N^{2s})\sum_{j=1}^{N/2}\big\|e^{-\kappa_0(1-x)/\varepsilon}\big\|^2_{L^2(I_j)}\\&\le C\,\varepsilon^{2(2-s)}(1+\varepsilon^4N^{2s})\int_{0}^{1-\lambda}e^{-2\kappa_0(1-x)/\varepsilon}\,dx\\&\le C\,\varepsilon^{2(2-s)}(1+\varepsilon^4N^{2s})e^{-2\kappa_0\lambda/\varepsilon}\\&\le C\,\varepsilon^{5-2s}(1+\varepsilon^4N^{2s})N^{-2(r+1-s)}.\\&\le C\,\varepsilon^{5-2s}N^{-2(r+1-s)}.\end{aligned} \tag{45}$$

Here, we have used $1 + \varepsilon^4 N^{2s} \leq 1$ for $s = 0, 1, 2$. Combining (43)–(45) proves (32).

Using the same line of reasoning, and invoking (29) and (30) together with (16) and (17), we obtain

$$\sum_{j=1}^{N} \frac{1}{\mu_j} \|\xi^2\|^2_{L^2(I_j)} \leq C(N^{-1} \ln N)^{2(r-1)},$$
$$\sum_{j=1}^{N} \frac{1}{\theta_j} \|\xi^1\|^2_{L^2(\partial I_j)} \leq C\left(\varepsilon^2 (N^{-1} \ln N)^{2r} + N^{-2r+1}\right) \leq CN^{-2r+1}.$$

This establishes (33) and (34).

Next, invoking the inverse trace inequality (30) and the regularity bounds (6), we obtain

$$\sum_{j=1}^{N} \frac{\varepsilon^2}{\theta_j} \|\xi_r^2\|^2_{L^2(\partial I_j)} \leq C \sum_{j=1}^{N} \varepsilon^2 k_j^{2r-3} \leq C\varepsilon N^{-2(r-1)}, \tag{46}$$

where we have used $\varepsilon \leq CN^{-1}$ and the mesh size $k_j \leq CN^{-1}$ and the definition of $\theta_j^{-1} \leq 1$ for $j = 1, \ldots, N$.

For the layer components, we have

$$\sum_{j=N/2+1}^{N} \frac{\varepsilon^2}{\theta_j} \|\xi_\ell^2\|^2_{L^2(\partial I_j)} \leq C\varepsilon^2 (N^{-1} \ln N)^{2(r-1)}. \tag{47}$$

Using the trace inequality (28) together with the stability bound (25) and the regularity property (6), we derive an estimate for the projection error of the layer function on the coarse region. Specifically, by using the exponential decay of the boundary layer component and summing over the fine-mesh region, this yields

$$\begin{aligned}
\sum_{j=1}^{N/2} \frac{\varepsilon^2}{\theta_j} \left\|\xi_\ell^2\right\|^2_{L^2(\partial I_j)} &\leq C \sum_{j=1}^{N/2} \frac{\varepsilon^2}{\theta_j} \left(\frac{1}{k_j} \left\|v_\ell''\right\|^2_{L^2(I_j)} + \left\|v_\ell''\right\|_{L^2(I_j)} \left\|v_\ell'''\right\|_{L^2(I_j)} + \frac{1}{k_j^5} \left\|v_\ell\right\|^2_{L^2(I_j)} \right) \\
&\leq C\, \varepsilon^2 \left(N\varepsilon N^{-2(r+1)} + N^{-2(r+1)} + (\varepsilon N)^5 N^{-2(r+1)} \right) \\
&\leq C\, \varepsilon^2 N^{-2(r+1)},
\end{aligned} \tag{48}$$

where the mesh-dependent bounds $\theta_j = 1,$ and $k_j = O(N^{-1}),$ for $j = 1, \ldots, N/2$, have been used. This completes the proof of (35).

From (6) and (17), together with the definition of θ_j and the trace–inverse inequality (30), we obtain

$$\sum_{j=1}^{N} \theta_j \left\|\xi_r^{(1)}\right\|^2_{L^2(\partial I_j)} \leq C\, N^{-2(r-1/2)} \tag{49}$$

and

$$\sum_{j=N/2+1}^{N} \theta_j \|\xi_\ell^{(1)}\|^2_{L^2(\partial I_j)} \leq C\varepsilon^2 (N^{-1} \ln N)^{2(r-1)} \tag{50}$$

Arguing as in (48), we obtain

$$\begin{aligned}
&\sum_{j=1}^{N/2} \theta_j \left\|\xi_\ell^{(1)}\right\|_{L^2(\partial I_j)}^2 \\
&\le C \sum_{j=1}^{N/2} \theta_j \left(k_j^{-1} \left\|v_\ell'\right\|_{L^2(I_j)}^2 + \left\|v_\ell'\right\|_{L^2(I_j)} \left\|v_\ell''\right\|_{L^2(I_j)} + k_j^{-3} \left\|v_\ell\right\|_{L^2(I_j)}^2 \right) \\
&\le C \left(N\varepsilon^3 N^{-2(r+1)} + \varepsilon N^{-2(r+1)} + N^2\varepsilon^5 N^{-2(r+1)} \right) \\
&\le C\, \varepsilon N^{-2(r+1)}.
\end{aligned} \tag{51}$$

Combining (49)–(51) yields (36).

Next, invoking (30), (10) and (6) and the definition of μ_j in (16), we obtain

$$\begin{aligned}
\sum_{j=1}^{N} \frac{\varepsilon^2}{\mu_j} \left\|(\xi_r^2)'\right\|_{L^2(\partial I_j)}^2 &\le C \left(\frac{\varepsilon^2}{N} N^{-2r+5} \right) |v_r|_{H^{r+1}(\Omega)}^2 \\
&\le C\, N^{-2(r-1)}.
\end{aligned} \tag{52}$$

Here, we have used the bounds $\mu_j^{-1} \le N^{-1}$ and $k_j \le CN^{-1}$ for $j = 1, \ldots, N$, which completes the proof of (37).

For the layer component v_ℓ, it follows from (29) that for $j = N/2, \ldots, N$, we have

$$\begin{aligned}
\left\|(\xi_\ell^2)'\right\|_{L^\infty(I_j)} &\le C\, k_j^{r-2} \left\|v_\ell^{(r+1)}\right\|_{L^\infty(I_j)} \\
&\le C\, \varepsilon^{r-2} (N^{-1} \ln N)^{r-2} \left\|\varepsilon^{1-r} e^{-\kappa_0(1-x)/\varepsilon}\right\|_{L^\infty(I_j)}.
\end{aligned}$$

Consequently

$$\sum_{j=N/2}^{N} \left\|(\xi_\ell^2)'\right\|_{L^\infty(I_j)} \le C\, \varepsilon^{-1} (N^{-1} \ln N)^{r-2}. \tag{53}$$

Therefore, the estimate (38) follows immediately.

By the trace inequality (28), the stability estimate (25), and the regularity bounds (6), we obtain

$$\begin{aligned}
&\sum_{j=1}^{N/2} \frac{\varepsilon^2}{\mu_j} \left\|(\xi_\ell^2)'\right\|_{L^2(\partial I_j)}^2 \\
&\le \sum_{j=1}^{N/2} \frac{\varepsilon^2}{\mu_j} \left(\|v_\ell'''\|_{L^2(\partial I_j)}^2 + \left\|(\mathcal{J}^{\mathrm{o}} v_\ell'')'\right\|_{L^2(\partial I_j)}^2 \right) \\
&\le \sum_{j=1}^{N/2} \frac{\varepsilon^2}{\mu_j} \left(\|v_\ell'''\|_{L^2(\partial I_j)}^2 + C k_j^{-3} \|\mathcal{J}^{\mathrm{o}} v_\ell''\|_{L^2(I_j)}^2 \right) \\
&\le \sum_{j=1}^{N/2} \frac{\varepsilon^2}{\mu_j} \left(\|v_\ell'''\|_{L^2(\partial I_j)}^2 + C k_j^{-3} \|v_\ell''\|_{L^2(I_j)}^2 \right)
\end{aligned}$$

$$\leq C \sum_{j=1}^{N/2} \frac{\varepsilon^2}{\mu_j} \Big(k_j^{-1} \|v_\ell'''\|_{L^2(I_j)}^2 + \|v_\ell'''\|_{L^2(I_j)} \|v_\ell''''\|_{L^2(I_j)} + k_j^{-3} \|v_\ell''\|_{L^2(I_j)}^2 \Big)$$
$$\leq C\, \varepsilon^2 N^{-1} \Big(N\varepsilon^{-2} \varepsilon N^{-2(r+1)} + \varepsilon^{-1} \varepsilon^{1/2} N^{-(r+1)} \varepsilon^{-2} \varepsilon^{1/2} N^{-(r+1)} + N^3 \varepsilon N^{-2(r+1)} \Big)$$
$$\leq C\, N^{-2(r+1)}. \tag{54}$$

Here, we use $k_j = O(N^{-1})$ for $j = 1, \ldots, N/2$. This completes the proof of (39).

For the remaining estimates, we use the bound $\mu_j^{-1} \leq CN^{-1}$ for $j = 1, \ldots, N$. By analogous arguments, for $s = 0, 1$, we obtain

$$\sum_{j=1}^{N} \frac{1}{\mu_j} \|\xi_r^s\|_{L^2(\partial I_j)}^2 \leq CN^{-1} \Big[N^{-2(r+1/2-s)} + (\varepsilon N^{-1} \ln N)^{2(r+1/2-s)} \Big] |v_r|_{H^{r+1}(\Omega)}^2$$
$$\leq CN^{-2(r+1-s)}. \tag{55}$$

For the layer component, we have the following for $s = 0, 1$:

$$\sum_{j=N/2+1}^{N} \frac{1}{\mu_j} \|\xi_\ell^s\|_{L^2(\partial I_j)}^2 \leq C \frac{\ln N}{N} \sum_{j=N/2+1}^{N} k_j^{2r+1-2s} |v_\ell|_{H^{r+1}(I_j)}^2$$
$$\leq C\varepsilon^{4-2s} (N^{-1} \ln N)^{2r+2-2s}. \tag{56}$$

Proceeding in the same manner, we also obtain the following for $s = 0, 1$:

$$\sum_{j=1}^{N/2} \frac{1}{\mu_j} \|\xi_\ell^s\|_{L^2(\partial I_j)}^2 \leq C \sum_{j=1}^{N/2} \frac{1}{\mu_j} \Big(k_j^{-1} \|v_\ell^{(s)}\|_{L^2(I_j)}^2 + \|v_\ell^{(s)}\|_{L^2(I_j)} \|v_\ell^{(s+1)}\|_{L^2(I_j)} \Big)$$
$$\leq C\varepsilon^{4-2s} N^{-2(r+3/2)}. \tag{57}$$

Consequently, combining (55)–(57) yields the assertions (40) and (41). The estimate (42) follows analogously. This completes the proof.

□

5. Error analysis

This section is devoted to the derivation of robust a priori error bounds for the WG-FEM measured in the energy norm (20). In particular, we establish convergence results that are robust with respect to the perturbation parameter.

Since the weak Galerkin formulation used here is intrinsically nonconforming, the error analysis cannot rely on standard Galerkin orthogonality. Instead, suitable error identities must be developed to facilitate the analysis. These identities are summarized in the lemma stated below and form the foundation of the subsequent estimates.

Lemma 5.1. *Let v denote the exact solution of* (1) *and let $\mathcal{J}v$ be the projection introduced in* (24)*. For any test function $\phi_N = \{\phi^o, \phi^\partial, \phi^g\} \in \mathcal{W}_N^o$, we have the following identities:*

$$\varepsilon(v^{(iv)}, \phi^o) = \varepsilon(D_w^2 \mathcal{J}v, D_w^2 \phi_N) + \mathcal{R}_1(v, \phi_N), \tag{58}$$

$$
\begin{aligned}
-((\kappa v'')', \phi^{\mathrm{o}}) - ((\eta v')', \phi^{\mathrm{o}}) &= \frac{1}{2}\Big((\kappa D_w(\mathcal{J}v), D_w^2\phi_N) - (\kappa D_w^2(\mathcal{J}v), D_w\phi_N)\Big) \\
&\quad + ((\eta - \frac{\kappa'}{2})\, D_w(\mathcal{J}v), D_w\phi) + \frac{1}{2}\kappa(1)v'(1)\phi^g(1) + \mathcal{R}_2(v,\phi_N) + \mathcal{R}_3(v,\phi_N),
\end{aligned} \tag{59}
$$

$$
(\rho v', \phi^{\mathrm{o}}) = (D_w^{\rho}(\mathcal{J}v), \phi^{\mathrm{o}}) + \mathcal{R}_4(v,\phi_N) \tag{60}
$$

$$
(\sigma v, \phi^{\mathrm{o}}) = (\sigma\mathcal{J}^0 v, \phi^{\mathrm{o}}) + \mathcal{R}_5(v,\phi_N). \tag{61}
$$

where the residual terms $\mathcal{R}_i(v,\phi_N)$, $i = 1,2,\ldots,5$ *are given by*

$$
\begin{aligned}
\mathcal{R}_1^1(v,\phi_N) &= -\varepsilon\langle\xi^2(v),\ (D\phi^{\mathrm{o}} - \phi^g)\mathbf{n}\rangle_{\mathcal{T}_N\setminus\{1\}} + \varepsilon\langle(\xi^2(v))',\ (\phi^{\mathrm{o}} - \phi^{\partial})\mathbf{n}\rangle, \\
&\quad - \varepsilon\zeta_1 D\phi^{\mathrm{o}}(1) + \varepsilon(D\phi^{\mathrm{o}} - \phi^g)(1)\mathcal{J}^0 v''(1),
\end{aligned} \tag{62}
$$

$$
\mathcal{R}_2(v,\phi_N) = \langle\kappa\xi^2(v), (\phi^{\mathrm{o}} - \phi^{\partial})\mathbf{n}\rangle + \frac{1}{2}\langle\kappa\xi^1(v), (\phi^g - D\phi^{\mathrm{o}})\mathbf{n}\rangle, \tag{63}
$$

$$
\mathcal{R}_3(v,\phi_N) = \langle(\eta - \frac{\kappa'}{2})\xi^1(v),\ (\phi^{\partial} - \phi^{\mathrm{o}})\boldsymbol{n}\rangle, \tag{64}
$$

$$
\mathcal{R}_4(v,\phi_N) = -(\xi(v),\ (\rho\phi^{\mathrm{o}})') \tag{65}
$$

$$
\mathcal{R}_5(v,\phi_N) = -(\sigma\xi(v), \phi^{\mathrm{o}}). \tag{66}
$$

Here, we have used $\langle\psi\mathbf{n}, u\rangle_{\mathcal{T}_N\setminus\{1\}} = \sum_{j=1}^{N-1}\langle\psi\mathbf{n}, u\rangle_{\partial I_j} - u(t_{N-1})\psi(t_{N-1}^+)$ *and the notation defined in* (31).

Proof. It follows from the definition of the weak second derivative (13) and an application of integration by parts that

$$
\begin{aligned}
(D_w^2\mathcal{J}v, D_w^2\phi_N)_{L^2(I_j)} &= (\phi^{\mathrm{o}}, (D_w^2\mathcal{J}v)'')_{L^2(I_j)} - \langle\phi^{\partial}, (D_w^2\mathcal{J}v)'\mathbf{n}\rangle_{\partial I_j} + \langle\phi^g\mathbf{n}, D_w^2\mathcal{J}v\rangle_{\partial I_j} \\
&= (D_w^2\mathcal{J}v, D^2\phi^{\mathrm{o}})_{L^2(I_j)} + \langle\phi^{\mathrm{o}}, (D_w^2\mathcal{J}v)'\mathbf{n}\rangle_{\partial I_j} \\
&\quad - \langle D\phi^{\mathrm{o}}\mathbf{n}, D_w^2\mathcal{J}v\rangle_{\partial I_j} \quad - \langle\phi^{\partial}, (D_w^2\mathcal{J}v)'\mathbf{n}\rangle_{\partial I_j} + \langle\phi^g\mathbf{n}, D_w^2\mathcal{J}v\rangle_{\partial I_j} \\
&= (\mathcal{J}^{\mathrm{o}}D^2v, D^2\phi^{\mathrm{o}})_{L^2(I_j)} + \langle\phi^{\mathrm{o}} - \phi^{\partial}, (\mathcal{J}^{\mathrm{o}}D^2v)'\mathbf{n}\rangle_{\partial I_j} \\
&\quad - \langle(D\phi^{\mathrm{o}} - \phi^g)\mathbf{n}, \mathcal{J}^{\mathrm{o}}D^2v\rangle_{\partial I_j} \\
&= (D^2v, D^2\phi^{\mathrm{o}})_{L^2(I_j)} + \langle\phi^{\mathrm{o}} - \phi^{\partial}, (\mathcal{J}^{\mathrm{o}}D^2v)'\mathbf{n}\rangle_{\partial I_j} \\
&\quad - \langle(D\phi^{\mathrm{o}} - \phi^g)\mathbf{n}, \mathcal{J}^{\mathrm{o}}D^2v\rangle_{\partial I_j},
\end{aligned} \tag{67}
$$

for any $\phi_N \in \mathcal{W}_N^{\mathrm{o}}$, where we have used (27) and the definition of the L^2-projection $\mathcal{J}^{\mathrm{o}}$.

Summing over all subintervals I_j, we obtain

$$
\begin{aligned}
\varepsilon(D_w^2\mathcal{J}v, D_w^2\phi_N) &= \varepsilon(D^2v, D^2\phi^{\mathrm{o}}) + \varepsilon\sum_{j=1}^{N}\langle\phi^{\mathrm{o}} - \phi^{\partial}, (\mathcal{J}^{\mathrm{o}}D^2v)'\mathbf{n}\rangle_{\partial I_j} \\
&\quad - \varepsilon(D\phi^{\mathrm{o}}(1) - \phi^g(1))\mathcal{J}^{\mathrm{o}}v''(1) - \varepsilon\langle(D\phi^{\mathrm{o}} - \phi^g)\mathbf{n}, \mathcal{J}^{\mathrm{o}}D^2v\rangle_{\mathcal{T}_N\setminus\{1\}}.
\end{aligned} \tag{68}
$$

Integration by parts yields

$$
\begin{aligned}
\varepsilon(v^{(iv)}, \phi^{\mathrm{o}}) &= \varepsilon(D^2v, D^2\phi^{\mathrm{o}}) - \varepsilon\zeta_1 D\phi^{\mathrm{o}}(1) - \varepsilon\langle D^2v, (D\phi^{\mathrm{o}} - \phi^g)\mathbf{n}\rangle_{\mathcal{T}_N\setminus\{1\}} \\
&\quad + \varepsilon\langle(D^2v)'\mathbf{n}, \phi^{\mathrm{o}} - \phi^{\partial}\rangle_{\partial I_j}\Big).
\end{aligned} \tag{69}
$$

Combining (68) and (69) gives (58).

Using the identity (26) of Lemma 4.1, it follows that for any $\phi_N = \{\phi^o, \phi^\partial, \phi^g\} \in \mathcal{W}_N^o$ and for each element $I_j \in \mathcal{T}_N$, one has

$$(D_w(\mathcal{J}v), D_w^2\phi_N)_{I_j} = (\mathcal{J}^o(Dv), D_w^2\phi_N)_{I_j}. \tag{70}$$

Invoking the definition of the weak second derivative and applying integration by parts on I_j, we obtain

$$(\mathcal{J}^o(Dv), D_w^2\phi_N)_{I_j} = (\phi^o, (\mathcal{J}^o(Dv))'')_{L^2(I_j)} - \langle \phi^\partial, (\mathcal{J}^o(Dv))'\mathbf{n}\rangle_{\partial I_j} + \langle \phi^g\mathbf{n}, \mathcal{J}^o(Dv)\rangle_{\partial I_j}.$$

Further integration by parts yields

$$(\phi^o, (\mathcal{J}^o(Dv))'')_{L^2(I_j)} = -(D\phi^o, (\mathcal{J}^o(Dv))')_{L^2(I_j)} + \langle \phi^o, (\mathcal{J}^o(Dv))'\mathbf{n}\rangle_{\partial I_j}.$$

Therefore

$$\begin{aligned}(\mathcal{J}^o(Dv), D_w^2\phi_N)_{I_j} = &-(D\phi^o, (\mathcal{J}^o(Dv))')_{L^2(I_j)} + \langle \phi^o - \phi^\partial, (\mathcal{J}^o(Dv))'\mathbf{n}\rangle_{\partial I_j} \\ &+ \langle \phi^g\mathbf{n}, \mathcal{J}^o(Dv)\rangle_{\partial I_j}.\end{aligned}$$

Finally, integrating by parts once more inside the element gives

$$-(D\phi^o, (\mathcal{J}^o(Dv))')_{L^2(I_j)} = (D^2\phi^o, \mathcal{J}^o(Dv))_{L^2(I_j)} - \langle D\phi^o\mathbf{n}, \mathcal{J}^o(Dv)\rangle_{\partial I_j},$$

which leads to the representation

$$\begin{aligned}(\mathcal{J}^o(Dv), D_w^2\phi_N)_{I_j} = &(D^2\phi^o, \mathcal{J}^o(Dv))_{L^2(I_j)} \\ &+ \langle (\mathcal{J}^o(Dv))', (\phi^o - \phi^\partial)\mathbf{n}\rangle_{\partial I_j} + \langle \mathcal{J}^o(Dv), (\phi^g - D\phi^o)\mathbf{n}\rangle_{\partial I_j}.\end{aligned} \tag{71}$$

Using the property of the projection operator, we obtain

$$(D^2\phi^o, \mathcal{J}^o(Dv))_{I_j} = (D^2\phi^o, Dv)_{I_j}. \tag{72}$$

From (70)–(72), we obtain

$$\begin{aligned}(\kappa D_w(\mathcal{J}v), D_w^2\phi_N)_{I_j} = &(\kappa D^2\phi^o, Dv)_{I_j} + \langle \kappa\mathcal{J}^o v'', (\phi^o - \phi^\partial)\mathbf{n}\rangle_{\partial I_j} \\ &+ \langle \kappa\mathcal{J}^o(Dv), (\phi^g - D\phi^o)\mathbf{n}\rangle_{\partial I_j}.\end{aligned} \tag{73}$$

Using (26) together with the definition of the weak derivative and an application of integration by parts on each subinterval I_j, we obtain

$$\begin{aligned}(D_w^2(\mathcal{J}v), D_w\phi)_{I_j} &= (\mathcal{J}^o v'', D_w\phi)_{I_j} \\ &= -(\phi^o, (\mathcal{J}^o v'')')_{I_j} + \langle \phi^\partial n, \mathcal{J}^o v''\rangle_{\partial I_j}.\end{aligned}$$

Using integration by parts, the expression above can be rewritten as

$$(D_w^2(\mathcal{J}v), D_w\phi)_{I_j} = ((\phi^o)', \mathcal{J}^o v'')_{I_j} - \langle (\phi^o - \phi^\partial)n, \mathcal{J}^o v''\rangle_{\partial I_j}.$$

Arguing as in the derivation of equation (72) above, it follows that

$$((\phi^o)', \mathcal{J}^o v'')_{I_j} = ((\phi^o)', v'')_{I_j}.$$

Consequently, we have

$$(\kappa D_w^2(\mathcal{J}v), D_w\phi)_{I_j} = (\kappa(\phi^{\mathrm{o}})', v'')_{I_j} - \langle \kappa(\phi^{\mathrm{o}} - \phi^{\partial})n, \mathcal{J}^{\mathrm{o}}v''\rangle_{\partial I_j}.$$

Combining this identity with (73), we arrive at

$$\begin{aligned}
&(\kappa D_w(\mathcal{J}v), D_w^2\phi)_{I_j} - (\kappa D_w^2(\mathcal{J}v), D_w\phi)_{I_j} \\
&= (\kappa(\phi^{\mathrm{o}})'', v')_{I_j} - (\kappa(\phi^{\mathrm{o}})', v'')_{I_j} + 2\langle \kappa\mathcal{J}^{\mathrm{o}}v'', (\phi^{\mathrm{o}} - \phi^{\partial})n\rangle_{\partial I_j} \\
&\quad + \langle \kappa\mathcal{J}^{\mathrm{o}}v', (\phi^g - (\phi^{\mathrm{o}})')n\rangle_{\partial I_j}.
\end{aligned}$$

Finally, summing over all elements $I_j \in \mathcal{T}$, we obtain the global identity

$$\begin{aligned}
&(\kappa D_w(\mathcal{J}^{\mathrm{o}}v), D_w^2\phi) - (\kappa D_w^2(\mathcal{J}v), D_w\phi) \\
&= (\kappa(\phi^{\mathrm{o}})'', v') - (\kappa(\phi^{\mathrm{o}})', v'') \\
&\quad + 2\langle \kappa\mathcal{J}^{\mathrm{o}}v'', (\phi^{\mathrm{o}} - \phi^{\partial})n\rangle + \langle \kappa\mathcal{J}^{\mathrm{o}}v', (\phi^g - (\phi^{\mathrm{o}})')n\rangle.
\end{aligned} \tag{74}$$

We consider the term $-((\kappa(x)v''(x))', \phi^{\mathrm{o}})_{I_j}$. Applying integration by parts twice on each interval I_j, we obtain

$$\begin{aligned}
-((\kappa v'')', \phi^{\mathrm{o}})_{I_j} &= (\kappa v'', (\phi^{\mathrm{o}})')_{I_j} - \langle \kappa v'', \phi^{\mathrm{o}}n\rangle_{\partial I_j} \\
&= -(v', (\kappa(\phi^{\mathrm{o}})')')_{I_j} + \langle \kappa v', (\phi^{\mathrm{o}})'n\rangle_{\partial I_j} - \langle \kappa v'', \phi^{\mathrm{o}}n\rangle_{\partial I_j}.
\end{aligned}$$

Collecting all contributions, we arrive at the symmetric representation

$$\begin{aligned}
-((\kappa v'')', \phi^{\mathrm{o}})_{I_j} = \frac{1}{2}\Big((\kappa v'', (\phi^{\mathrm{o}})')_{I_j} - (v', (\kappa(\phi^{\mathrm{o}})')')_{I_j}\Big) \\
- \langle \kappa v'', \phi^{\mathrm{o}}n\rangle_{\partial I_j} + \frac{1}{2}\langle \kappa v', (\phi^{\mathrm{o}})'n\rangle_{\partial I_j}.
\end{aligned}$$

Summing over all intervals I_j and using the identities

$$\sum_{j=1}^{N}\langle \kappa v'', \phi^{\partial}n\rangle_{\partial I_j} = 0, \qquad \sum_{j=1}^{N}\langle \kappa v', \phi^g n\rangle_{\partial I_j} = \kappa(1)v'(1)\phi^g(1),$$

we obtain

$$\begin{aligned}
-((\kappa v'')', \phi^{\mathrm{o}}) = \frac{1}{2}\Big((\kappa v'', (\phi^{\mathrm{o}})') - (v', \kappa(\phi^{\mathrm{o}})'')\Big) - (v', \frac{\kappa'}{2}(\phi^{\mathrm{o}})') \\
- \langle \kappa v'', (\phi^{\mathrm{o}} - \phi^{\partial})n\rangle + \frac{1}{2}\langle \kappa v', ((\phi^{\mathrm{o}})' - \phi^g)n\rangle + \frac{1}{2}\kappa(1)v'(1)\phi^g(1).
\end{aligned} \tag{75}$$

Combining (74) and (75), we have

$$\begin{aligned}
-((\kappa v'')', \phi^{\mathrm{o}}) = \frac{1}{2}\Big((\kappa D_w^2(\mathcal{J}v), D_w\phi) - (\kappa D_w(\mathcal{J}^{\mathrm{o}}v), D_w^2\phi)\Big) \\
- \langle \kappa(v'' - \mathcal{J}^{\mathrm{o}}v''), (\phi^{\mathrm{o}} - \phi^{\partial})n\rangle + \frac{1}{2}\langle \kappa(v' - \mathcal{J}^{\mathrm{o}}v'), ((\phi^{\mathrm{o}})' - \phi^g)n\rangle.
\end{aligned} \tag{76}$$

$$- (v', \frac{\kappa'}{2}(\phi^{\mathrm{o}})') + \frac{1}{2}\kappa(1)v'(1)\phi^{g}(1).$$

Invoking (26) together with the definition of the weak derivative (14), for any test function $\phi_N \in \mathcal{W}_N^{\mathrm{o}}$, we obtain

$$\begin{aligned}(-\tfrac{\kappa'}{2}D_w\mathcal{J}v, D_w\phi_N)_{L^2(I_j)} &= (-\tfrac{\kappa'}{2}\mathcal{J}^{\mathrm{o}}Dv, D_w\phi_N)_{L^2(I_j)}\\ &= -(\phi^{\mathrm{o}}, (-\tfrac{\kappa'}{2}\mathcal{J}^{\mathrm{o}}Dv)')_{L^2(I_j)} + \langle\phi^{\partial}, (-\tfrac{\kappa'}{2}\mathcal{J}^{\mathrm{o}}Dv)\mathbf{n}\rangle_{\partial I_j}\\ &= (D\phi^{\mathrm{o}}, -\tfrac{\kappa'}{2}\mathcal{J}^{\mathrm{o}}Dv)_{L^2(I_j)} - \langle\phi^{\mathrm{o}} - \phi^{\partial}, (-\tfrac{\kappa'}{2}\mathcal{J}^{\mathrm{o}}Dv)\mathbf{n}\rangle_{\partial I_j}\\ &= (-\tfrac{\kappa'}{2}Dv, D\phi^{\mathrm{o}})_{L^2(I_j)} - \langle\phi^{\mathrm{o}} - \phi^{\partial}, (-\tfrac{\kappa'}{2}\mathcal{J}^{\mathrm{o}}Dv)\mathbf{n}\rangle_{\partial I_j}.\end{aligned}$$

Thus, summing over all subintervals I_j, we obtain

$$(Dv, \tfrac{\kappa'}{2}D\phi^{\mathrm{o}}) = (\tfrac{\kappa'}{2}D_w\mathcal{J}v, D_w\phi_N) - \sum_{j=1}^{N}\langle\phi^{\mathrm{o}} - \phi^{\partial}, (-\tfrac{\kappa}{2}\mathcal{J}^{\mathrm{o}}Dv)\mathbf{n}\rangle_{\partial I_j}. \tag{77}$$

By integration by parts, we have

$$-((\eta v')', \phi^{\mathrm{o}})_{L^2(I_j)} = (\eta Dv, D\phi^{\mathrm{o}})_{L^2(I_j)} - \langle\eta Dv\,\mathbf{n}, \phi^{\mathrm{o}}\rangle_{\partial I_j}.$$

Summing over all intervals I_j and using the identity $\sum_{j=1}^{N}\langle\eta v', \phi^{\partial}\mathbf{n}\rangle_{\partial I_j} = 0$, one has

$$-((\eta v')', \phi^{\mathrm{o}}) = (\eta Dv, D\phi^{\mathrm{o}}) - \sum_{j=1}^{N}\langle\eta Dv, (\phi^{\mathrm{o}} - \phi^{\partial})\mathbf{n}\rangle_{\partial I_j}$$

Combining the identity above with Eq (77) and replacing the coefficient $\frac{\kappa}{2}$ by η, we obtain the following error equation:

$$-((\eta v')', \phi^{\mathrm{o}}) = (\eta D_w\mathcal{J}v, D_w\phi_N) - \sum_{j=1}^{N}\langle(\phi^{\mathrm{o}} - \phi^{\partial})\,\mathbf{n}, \eta(\mathcal{J}^{\mathrm{o}}Dv - Dv)\rangle_{\partial I_j}. \tag{78}$$

A direct combination of (76)–(78) leads to the identity in (59). Similarly, by using the weak convection derivative (15), applying integration by parts, and using the boundary projection $\mathcal{J}^{\partial}$, we obtain

$$\begin{aligned}(D_w^{\rho}(\mathcal{J}v), \phi^{\mathrm{o}}) &= -(\mathcal{J}^{\mathrm{o}}v, (\rho\phi^{\mathrm{o}})') + \sum_{j=1}^{N}\langle\mathcal{J}^{\partial}v, \rho\,\mathbf{n}\,\phi^{\mathrm{o}}\rangle_{\partial I_j}\\ &= -(\mathcal{J}^{\mathrm{o}}v, (\rho\phi^{\mathrm{o}})') + \sum_{j=1}^{N}\langle v, \rho\,\mathbf{n}\,\phi^{\mathrm{o}}\rangle_{\partial I_j},\end{aligned}$$

where we have used the definition of $\mathcal{J}^{\partial}$.

On the other hand, integration by parts yields

$$(\rho v', \phi^{\mathrm{o}}) = -(v, (\rho\phi^{\mathrm{o}})') + \sum_{j=1}^{N}\langle v, \rho\,\mathbf{n}\,\phi^{\mathrm{o}}\rangle_{\partial I_j}.$$

Consequently, comparing the identities above, we arrive at

$$(\rho v', \phi^{\mathrm{o}}) = (D_w^{\rho}(\mathcal{J}v), \phi^{\mathrm{o}}) + (\mathcal{J}^{\mathrm{o}}v - v, (\rho\phi^{\mathrm{o}})'),$$

which shows (60). The result in (61) is straightforward, and hence the proof is concluded. □

The following theorem establishes an a priori estimate for the discretization error $e_D := v_N - \mathcal{J}v$ measured in the discrete H^2–energy norm $\|\cdot\|_{\mathcal{D}}$.

Theorem 5.2. *Let $\mathcal{J}v$ denote the projection of the exact solution $v \in H^{r+1}(\Omega)$ of Problem* (1)*, and let v_N be the weak Galerkin finite element solution obtained from* (18) *on a Shishkin mesh. Then the discretization error e_D satisfies the estimate*

$$\|e_D\|_{\mathcal{D}} \leq C(N^{-1}\ln N)^{r-1},$$

where $C > 0$ is a constant independent of both ε and the mesh parameter N.

Proof. Considering (58)–(61) and adding stabilization terms gives

$$\begin{aligned}\mathcal{B}(\mathcal{J}v, \phi_N) = (h, \phi^{\mathrm{o}}) + \mathcal{R}_1^1(v, \phi_N) + \mathcal{R}_2(v, \phi_N) + \mathcal{R}_3(v, \phi_N)\\ + \mathcal{R}_4(v, \phi_N) + \mathcal{R}_5(v, \phi_N) + S(\mathcal{J}v, \phi_N).\end{aligned} \tag{79}$$

Finally, subtracting the weak Galerkin equation (18) from (79) yields the error equation

$$\begin{aligned}\mathcal{B}(e_D, \phi_N) &= \varepsilon\zeta_1(\phi^g - D\phi^{\mathrm{o}})(1) - \varepsilon(\phi^g - D\phi^{\mathrm{o}})\mathcal{J}^{\mathrm{o}}v''(1) + \varepsilon\langle(v'' - \mathcal{J}^{\mathrm{o}}v'')', (\phi^{\mathrm{o}} - \phi^{\partial})\mathbf{n}\rangle\\ &\quad + \varepsilon\langle(\phi^g - D\phi^{\mathrm{o}})\mathbf{n}, v'' - \mathcal{J}^{\mathrm{o}}v''\rangle_{\mathcal{T}_N\setminus\{1\}} + \mathcal{R}_2(v, \phi_N) + \mathcal{R}_3(v, \phi_N)\\ &\quad + \mathcal{R}_4(v, \phi_N) + \mathcal{R}_5(v, \phi_N) + S(\mathcal{J}v, \phi_N)\\ &= \mathcal{R}_1(v, \phi_N) + \mathcal{R}_2(v, \phi_N) + \mathcal{R}_3(v, \phi_N)\\ &\quad + \mathcal{R}_4(v, \phi_N) + \mathcal{R}_5(v, \phi_N) + S(\mathcal{J}v, \phi_N),\end{aligned} \tag{80}$$

where $\mathcal{R}_1(v, \phi_N) = -\varepsilon\langle(\phi^g - D\phi^{\mathrm{o}})\mathbf{n}, v'' - \mathcal{J}^{\mathrm{o}}v''\rangle + \varepsilon\langle(v'' - \mathcal{J}^{\mathrm{o}}v'')', (\phi^{\mathrm{o}} - \phi^{\partial})\mathbf{n}\rangle$.

Substituting $\phi_N = e_D$ into the error equation (80) yields

$$\mathcal{B}(e_D, e_D) = \mathcal{R}(v, e_D) + S(\mathcal{J}v, e_D), \tag{81}$$

where

$$\mathcal{R}(v, e_D) := \mathcal{R}_1(v, e_D) + \mathcal{R}_2(v, e_D) + \mathcal{R}_3(v, e_D) + \mathcal{R}_4(v, e_D) + \mathcal{R}_5(v, e_D).$$

Invoking the coercivity estimate (23) together with (81), we obtain

$$\|e_D\|_{\mathcal{D}}^2 \leq \mathcal{R}(v, e_D) + S(\mathcal{J}v, e_D). \tag{82}$$

We now proceed to estimate each term that appears in (82) separately. We begin with the contribution of the term $\mathcal{R}_1(v, e_D)$.

From the definition (62) of $\mathcal{R}_1(v, e_D)$, we write

$$\begin{aligned}|\mathcal{R}_1(v, e_D)| &\leq \varepsilon\left|\langle\xi^2, ((e_D^{\mathrm{o}})' - e_D^{\partial})n\rangle\right| + \varepsilon\left|\langle(\xi^2)', (e_D^{\mathrm{o}} - e_D^{\partial})n\rangle\right|\\ &=: \mathcal{R}_1^1(v, e_D) + \mathcal{R}_1^2(v, e_D).\end{aligned} \tag{83}$$

It follows from the Cauchy–Schwarz inequality and the estimates (35) of Lemma 4.3 that

$$\begin{aligned}\mathcal{R}_1^1(v, e_D) &\le \varepsilon \sum_{j=1}^{N} \|\xi^2\|_{L^2(\partial I_j)} \|(e_D^{\mathrm{o}})' - e_D^{\partial}\|_{L^2(\partial I_j)} \\ &\le C\bigg(\sum_{j=1}^{N} \frac{\varepsilon^2}{\theta_j} \left\|\xi^2\right\|_{L^2(\partial I_j)}^2 \bigg)^{\frac{1}{2}} \bigg(\sum_{j=1}^{N} \theta_j \left\|(e_D^{\mathrm{o}})' - e_D^{\partial}\right\|_{L^2(\partial I_j)}^2 \bigg)^{\frac{1}{2}} \\ &\le C\,(\varepsilon^{\frac{1}{2}} N^{-1} \ln N)^{r-1}\, s_d^{1/2}(e_D, e_D) \\ &\le C\,\varepsilon^{\frac{1}{2}} (N^{-1} \ln N)^{r-1}\, \|e_D\|_{\mathcal{D}}.\end{aligned} \tag{84}$$

Combining the Cauchy–Schwarz inequality with the Hölder inequality, we arrive at

$$\begin{aligned}\mathcal{R}_1^2(v, e_D) \le{}& \varepsilon \sum_{j=1}^{N} \|(\xi_r^2)'\|_{L^2(\partial I_j)} \|e_D^{\mathrm{o}} - e_D^{\partial}\|_{L^2(\partial I_j)} \\ &+ \varepsilon \sum_{j=1}^{N/2-1} \|(\xi_{\ell_1}^2)'\|_{L^2(I_j)} \|e_D^{\mathrm{o}} - e_D^{\partial}\|_{L^2(\partial I_j)} \\ &+ \varepsilon \sum_{j=N/2}^{N} \|(\xi_{\ell_1}^2)'\|_{L^\infty(\partial I_j)} \|e_D^{\mathrm{o}} - e_D^{\partial}\|_{L^1(\partial I_j)} \\ \le{}& C\bigg(\sum_{j=1}^{N} \frac{\varepsilon^2}{\mu_j} \|(\xi_r^2)'\|_{L^2(\partial I_j)}^2 \bigg)^{1/2} \bigg(\sum_{j=1}^{N} \mu_j \|e_D^{\mathrm{o}} - e_D^{\partial}\|_{L^2(\partial I_j)}^2 \bigg)^{1/2} \\ &+ \bigg(\sum_{j=1}^{N/2-1} \frac{\varepsilon^2}{\mu_j} \|(\xi_\ell^2)'\|_{L^2(\partial I_j)}^2 \bigg)^{1/2} \bigg(\sum_{j=1}^{N/2-1} \mu_j \|e_D^{\mathrm{o}} - e_D^{\partial}\|_{L^2(\partial I_j)}^2 \bigg)^{1/2} \\ &+ C\varepsilon^2 \bigg(\sum_{j=N/2}^{N} \|(\xi_\ell^2)'\|_{L^\infty(I_j)}^2 \mu_j^{-1} \bigg)^{1/2} \bigg(\sum_{j=N/2}^{N} 2\mu_j \|e_D^{\mathrm{o}} - e_D^{\partial}\|_{L^2(\partial I_j)}^2 \bigg)^{1/2}.\end{aligned}$$

Here, we have used $\|(\xi_\ell^2)'\|_{L^\infty(\partial I_j)} \le \|(\xi_\ell^2)'\|_{L^\infty(I_j)}$ since $v^{(3)}, (\mathcal{J}^{\mathrm{o}} v^{(2)})' \in C(I_j)$, and $\|e_D^{\mathrm{o}} - e_D^{\partial}\|_{L^1(\partial I_j)} \le \sqrt{2}\, \|e_D^{\mathrm{o}} - e_D^{\partial}\|_{L^2(\partial I_j)}$.

Using Lemma 4.3 together with the definition of μ_j, we obtain

$$\begin{aligned}&\mathcal{R}_1^2(v, e_D) \\ &\le C\Big(N^{-(r-1)} + N^{-(r+1)} + (N^{-1} \ln N)^{r-1} \Big) s_d^{1/2}(e_D, e_D) \\ &\le C\,(N^{-1} \ln N)^{r-1}\, \|e_D\|_{\mathcal{D}},\end{aligned} \tag{85}$$

where we have used $\varepsilon (N^{-1} \ln N)^{r-3/2} \le (N^{-1} \ln N)^{r-1}$ due to the assumption that $\varepsilon \le C N^{-1}$.

Next, we estimate the consistency term $\mathcal{R}_2(v, e_D)$. From (63) and the Cauchy–Schwarz inequality, we obtain

$$|\mathcal{R}_2(v, e_D)| \le C \|\kappa\|_{L^\infty(\Omega)} \sum_{j=1}^{N} \Big(\|\xi^2\|_{L^2(\partial I_j)} \|e_D^0 - e_D^{\partial}\|_{L^2(\partial I_j)}$$

$$+ \|\xi^1\|_{L^2(\partial I_j)}\|e_D^g - (e_D^0)'\|_{L^2(\partial I_j)}\Big)$$
$$\le C\Big(\sum_{j=1}^{N}\frac{1}{\mu_j}\|\xi^2\|^2_{L^2(\partial I_j)}\Big)^{1/2}\Big(\sum_{j=1}^{N}\mu_j\|e_D^0 - e_D^\partial\|^2_{L^2(\partial I_j)}\Big)^{1/2}$$
$$+ C\Big(\sum_{j=1}^{N}\frac{1}{\theta_j}\|\xi^1\|^2_{L^2(\partial I_j)}\Big)^{1/2}\Big(\sum_{j=1}^{N}\theta_j\|(e_D^0)' - e_D^g\|^2_{L^2(\partial I_j)}\Big)^{1/2}.$$

Using the interpolation estimates of Lemma 4.3, we conclude that

$$|\mathcal{R}_2(v, e_D)| \le C(N^{-1}\ln N)^{r-1}\, s_d^{1/2}(v, v).$$

Similarly, for $\mathcal{R}_3(v, e_D)$, we have

$$|\mathcal{R}_3(v, e_D)| \le C\|\eta - \frac{\kappa'}{2}\|_{L^\infty(\Omega)}\sum_{j=1}^{N}\|\xi^1\|_{L^2(\partial I_j)}\|e_D^{\mathrm{o}} - e_D^\partial\|_{L^2(\partial I_j)}$$
$$\le C\Big(\sum_{j=1}^{N}\frac{1}{\mu_j}\|\xi^1\|^2_{L^2(\partial I_j)}\Big)^{1/2}\Big(\sum_{j=1}^{N}\mu_j\|e_D^{\mathrm{o}} - e_D^\partial\|^2_{L^2(\partial I_j)}\Big)^{1/2}$$
$$\le CN^{-r}\|e_D\|_{\mathcal{D}}. \tag{86}$$

Next, combining $\mathcal{R}_4$ and $\mathcal{R}_5$, and using (65) and (66), we write

$$\mathcal{R}_4(v, e_D) + \mathcal{R}_5(v, e_D) = (\xi, \rho(e_D^{\mathrm{o}})') - (\xi, (\sigma - \rho')e_D^{\mathrm{o}}) =: \mathcal{G}(v, e_D).$$

Introducing the local average

$$\hat{\rho}\big|_{I_j} = \frac{1}{k_j}\int_{I_j}\rho(x)\,dx,$$

and using Lemma 4.3 together with an inverse inequality, we obtain

$$|\mathcal{G}(v, e_D)| \le |(\xi, (\rho - \hat{\rho})(e_D^{\mathrm{o}})')| + |(\xi, (\sigma - \rho')e_D^{\mathrm{o}})| \tag{87}$$
$$\le C\sum_{j=1}^{N}\Big(k_j\|\rho'\|_{L^\infty(I_j)}\|\xi\|_{L^2(I_j)}k_j^{-1}\|e_D^{\mathrm{o}}\|_{L^2(I_j)} + \|\xi\|_{L^2(I_j)}\|e_D^{\mathrm{o}}\|_{L^2(I_j)}\Big)$$
$$\le C\|\xi\|\|(\sigma - \rho'/2)^{1/2}e_D^{\mathrm{o}}\|$$
$$\le CN^{-(r+1)}\|e_D\|_{\mathcal{D}}.$$

The estimate (87) yields

$$\mathcal{R}_4(v, e_D) + \mathcal{R}_5(v, e_D) \le CN^{-(r+1)}\|e_D\|_{\mathcal{D}}. \tag{88}$$

Combining (84)–(88), we infer

$$\big|\mathcal{R}(v, e_D)\big| \le C(N^{-1}\ln N)^{r-1}\|e_D\|_{\mathcal{D}}. \tag{89}$$

Lastly, we estimate the stabilization term $s_d(\mathcal{J}v, e_D)$. By the Cauchy–Schwarz inequality, we have

$$\begin{aligned}
|s_d(\mathcal{J}v, e_D)| &\le \sum_{j=1}^{N} \Big(\theta_j \|(\mathcal{J}^{\mathrm{o}}v)' - \mathcal{J}^g v\|_{L^2(\partial I_j)} \|(e_D^{\mathrm{o}})' - e_D^g\|_{L^2(\partial I_j)} \\
&\qquad + \mu_j \|\mathcal{J}^{\mathrm{o}}v - \mathcal{J}^{\partial}v\|_{L^2(\partial I_j)} \|e_D^{\mathrm{o}} - e_D^{\partial}\|_{L^2(\partial I_j)}\Big) \\
&= \sum_{j=1}^{N} \Big(\theta_j \|\xi^{(1)}\|_{L^2(\partial I_j)} \|(e_D^{\mathrm{o}})' - e_D^g\|_{L^2(\partial I_j)} \\
&\qquad + \mu_j \|\xi\|_{L^2(\partial I_j)} \|e_D^{\mathrm{o}} - e_D^{\partial}\|_{L^2(\partial I_j)}\Big) \\
&\le C\bigg(\sum_{j=1}^{N} \theta_j \|\xi^{(1)}\|^2_{L^2(\partial I_j)}\bigg)^{1/2} \bigg(\sum_{j=1}^{N} \theta_j \|(e_D^{\mathrm{o}})' - e_D^g\|^2_{L^2(\partial I_j)}\bigg)^{1/2} \\
&\quad + C\bigg(\sum_{j=1}^{N} \mu_j \|\xi\|^2_{L^2(\partial I_j)}\bigg)^{1/2} \bigg(\sum_{j=1}^{N} \mu_j \|e_D^{\mathrm{o}} - e_D^{\partial}\|^2_{L^2(\partial I_j)}\bigg)^{1/2} \\
&\le CN^{-r+1/2} \|e_D\|_{\mathcal{D}},
\end{aligned} \tag{90}$$

where (36) and (42) of Lemma 4.3 have been used.

By an analogous argument, we also obtain

$$|s_c(\mathcal{J}v, e_D)| \le CN^{-(r+1/2)} \|e_D\|_{\mathcal{D}}. \tag{91}$$

Combining (89)–(91) yields the asserted estimate, and the proof is complete. □

We are now ready to present the principal result of this study, which establishes a uniform a priori error bound for the WG-FEM in the discrete energy norm (21).

Theorem 5.3. *Let v be the solution of* (1)*, and let v_N denote the WG-FEM approximation obtained from* (18) *on a Shishkin mesh. Then we have*

$$\|v - v_N\|_{\mathcal{D}} \le C(N^{-1} \ln N)^{r-1}.$$

Proof. Decompose the error as

$$v - v_N = \xi - e_D,$$

where $\xi := v - \mathcal{J}v$ is the projection error and $e_D := v_N - \mathcal{J}v$ is the discrete error. The estimate for e_D follows directly from Theorem 5.2 as follows:

$$\|e_D\|_{\mathcal{D}} \le C(N^{-1} \ln N)^{r-1}. \tag{92}$$

The discretization error has already been bounded in Theorem 5.2. It remains to control the projection error ξ in the discrete energy norm.

By the definition of the norm (21), we have

$$\begin{aligned}
\|\xi\|^2_{\mathcal{D}} = \varepsilon \|(v - \mathcal{J}^{\mathrm{o}}v)''\|^2 + \|(v - \mathcal{J}^{\mathrm{o}}v)'\|^2 + \|v - \mathcal{J}^{\mathrm{o}}v\|^2 + \frac{1}{2}\kappa(1)(\xi^g(1))^2 \\
+ |\xi|^2_{\rho} + s_d(\xi, \xi),
\end{aligned} \tag{93}$$

where we have used $\|D_w(v - \mathcal{J}^{\mathrm{o}}v)\| = \|(v - \mathcal{J}^{\mathrm{o}}v)'\|$ since $(v - \mathcal{J}^{\mathrm{o}}v)' \in C(I_j)$ for each subinterval I_j. We estimate each term on the right-hand side separately.

From the approximation estimate (32) of Lemma 4.3, it follows that

$$\begin{aligned} \varepsilon\|(v - \mathcal{J}^{\mathrm{o}}v)''\|^2 &\le C\,\varepsilon^2(N^{-1}\ln N)^{2(r-1)} + \varepsilon N^{-2(r-1)}, \\ \|(v - \mathcal{J}^{\mathrm{o}}v)'\|^2 &\le C(\varepsilon^3(N^{-1}\ln N)^{2r} + N^{-2r}), \\ \|v - \mathcal{J}^{\mathrm{o}}v\|^2 &\le C(\varepsilon^5(N^{-1}\ln N)^{2(r+1)} + N^{-2(r+1)}). \end{aligned} \tag{94}$$

It remains to estimate the stabilization and boundary contributions. From the definition of the projection operator, it follows that

$$\xi^g(1) = v'(1) - \mathcal{J}^g v(1) = 0. \tag{95}$$

Moreover, we observe that

$$|\xi|_\rho^2 = s_c(\mathcal{J}v, \mathcal{J}v) - \frac{1}{2}\langle \rho\mathbf{n}(\mathcal{J}^{\mathrm{o}}v - \mathcal{J}^{\partial}v), \mathcal{J}^{\mathrm{o}}v - \mathcal{J}^{\partial}v\rangle.$$

Invoking the estimates (90) and (91), we obtain

$$s_d(\xi, \xi) \le CN^{-2r+1}, \qquad |\xi|_\rho^2 \le CN^{-2r+1}. \tag{96}$$

Substituting (94) and (95) together with (96) into (93) yields

$$\|\xi\|_{\mathcal{D}}^2 \le CN^{-2r+1}. \tag{97}$$

Finally, combining (92) and (97), and applying the triangle inequality, we arrive at the desired estimate. This completes the proof. □

6. Numerical experiments

This section presents a series of numerical experiments designed to validate the theoretical error estimates and to illustrate the robustness of the proposed method with respect to the perturbation parameter. All computations are performed on the Shishkin mesh introduced in Section 2. The arising integrals are approximated by means of the five-point Gauss quadrature rule.

To assess the convergence behavior, we compute the observed order of convergence (OC) defined by

$$\mathrm{OC} = \frac{\ln(E_N/E_{2N})}{\ln(2\ln(N)/\ln(2N))},$$

where $E_N := \|v - v_N\|$ denotes the numerical error between the exact solution v and the WG-FEM approximation v_N obtained from (18) on the Shishkin mesh with N elements.

Example 6.1. *We consider a linear problem with constant coefficients [22]*

$$\varepsilon v^{(4)}(x) - v^{(3)}(x) - v''(x) + v'(x) + v(x) = h(x), \quad x \in [0, 1], \tag{98}$$

subject to the boundary conditions

$$v(0) = v(1) = v'(0) = v''(1) = 0.$$

The source term $h(x)$ is constructed in such a way that the problem admits the exact solution

$$v(x) = Ax^3 + Bx^2 + Cx + \varepsilon^2 \frac{e^{-1/\varepsilon} - e^{-(1-x)/\varepsilon}}{1 - e^{-1/\varepsilon}},$$

with

$$A = -\frac{\varepsilon^2}{2} + \frac{\varepsilon e^{-1/\varepsilon}}{2\left(1 - e^{-1/\varepsilon}\right)} + \frac{1}{4\left(1 - e^{-1/\varepsilon}\right)},$$

$$B = \frac{3}{2}\varepsilon^2 - \frac{3\varepsilon e^{-1/\varepsilon}}{2\left(1 - e^{-1/\varepsilon}\right)} - \frac{1}{4\left(1 - e^{-1/\varepsilon}\right)},$$

$$C = \frac{\varepsilon e^{-1/\varepsilon}}{1 - e^{-1/\varepsilon}}.$$

Figure 1 illustrates the solution $v(x)$ and its second derivative $v''(x)$ for a singularly perturbed problem with $\varepsilon = 10^{-4}$. The figure shows that $v''(x)$ has a steep gradient within the boundary layer. The second derivative attains a pronounced peak near $x = 1$, reflecting the high curvature of the solution in the layer region. This behavior confirms the presence of a thin boundary layer, while the solution remains smooth and slowly varying in the remainder of the domain. The observed boundary layer behavior is consistent with the theoretical analysis of singularly perturbed differential equations and demonstrates the necessity of resolving the layer accurately for small values of ε.

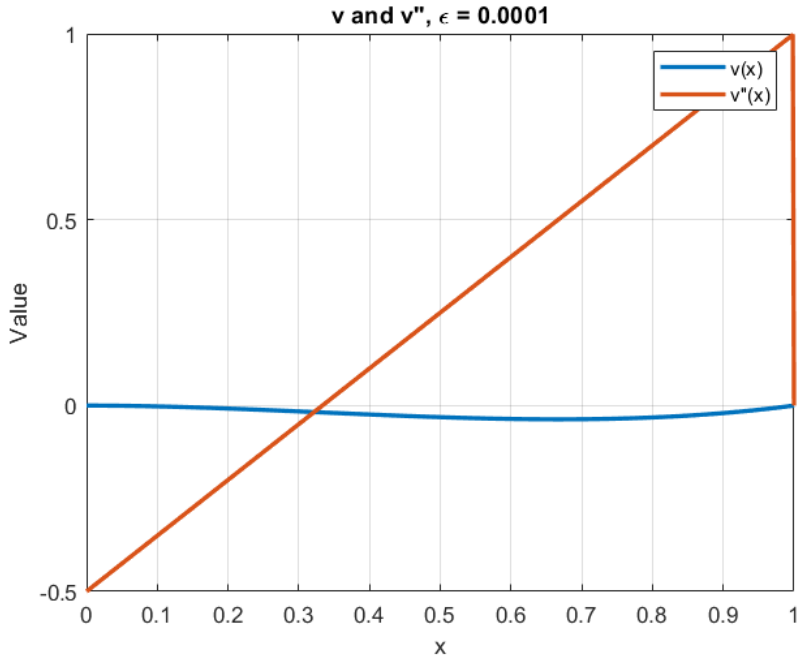

Figure 1. The solution $v(x)$ and its second derivative $v''(x)$ for $\varepsilon = 10^{-4}$. The top panel shows $v(x)$ with a sharp variation near $x = 1$ (the boundary layer). The bottom panel shows $v''(x)$, highlighting the steep gradient within the boundary layer.

Initially, we present the error estimates and examine the corresponding OC in the energy norm for the parameter values $\varepsilon = 10^{-2}, 10^{-4}, 10^{-8}$, as summarized in Table 1. Analysis of these results

indicates that the observed convergence rates are consistent with the theoretical predictions established in Theorem 5.3, thereby providing numerical validation of the theoretical error bounds.

Table 1. The errors in the enrgy norm and OC for the values of $\varepsilon = 10^{-2}$, 10^{-4}, and 10^{-8}.

		10^{-2}		10^{-4}		10^{-8}	
	N	$\|\|v - v_N\|\|_{\mathcal{D}}$	OC	$\|\|v - v_N\|\|_{\mathcal{D}}$	OC	$\|\|v - v_N\|\|_{\mathcal{D}}$	OC
	16	2.1432e−02	-	2.1450e−02	-	2.1410e−02	-
	32	1.3631e−02	0.962	1.3643e−02	0.962	1.3618e−02	0.962
	64	8.2738e−03	0.979	8.2810e−03	0.979	8.2660e−03	0.979
$\mathbb{P}_2$	128	4.8571e−03	0.989	4.8613e−03	0.989	4.8525e−03	0.989
	256	2.7840e−03	0.994	2.7864e−03	0.994	2.7814e−03	0.994
	512	1.5666e−03	0.999	1.5679e−03	0.999	1.5651e−03	0.999
	16	1.3203e−03	-	1.2947e−03	-	1.3048e−03	-
	32	5.2480e−04	1.960	5.1470e−04	1.962	5.1869e−04	1.961
	64	1.9122e−04	1.974	1.8755e−04	1.975	1.8901e−04	1.976
$\mathbb{P}_3$	128	6.5414e−05	1.981	6.4163e−05	1.982	6.4662e−05	1.983
	256	2.1459e−05	1.987	2.1048e−05	1.988	2.1212e−05	1.989
	512	6.7882e−06	1.993	6.6583e−06	1.994	6.7102e−06	1.999
	16	6.5003e−05	-	6.3802e−05	-	6.4301e−05	-
	32	1.6163e−05	2.960	1.5861e−05	2.962	1.5985e−05	2.961
	64	3.5279e−06	2.977	3.4620e−06	2.978	3.4890e−06	2.976
$\mathbb{P}_4$	128	7.0536e−07	2.985	6.9209e−07	2.986	6.9749e−07	2.985
	256	1.3205e−07	2.990	1.2956e−07	2.991	1.3057e−07	2.990
	512	2.3478e−08	2.995	2.3036e−08	2.996	2.3216e−08	2.998

Table 2. The energy errors using $N = 128$ and the elements $\mathbb{P}_2$, $\mathbb{P}_3$, and $\mathbb{P}_4$ for various values of ε.

ε	$k = 2$	$k = 3$	$k = 4$
10^{-2}	4.8571e−03	6.5414e−05	7.0536e−07
10^{-3}	4.8613e−03	6.4163e−05	6.9209e−07
10^{-4}	4.8527e−03	6.4161e−05	6.9211e−07
10^{-5}	4.8523e−03	6.4465e−05	6.9507e−07
10^{-6}	4.8526e−03	6.4560e−05	6.9610e−07
10^{-7}	4.8524e−03	6.4564e−05	6.9708e−07
10^{-8}	4.8525e−03	6.4660e−05	6.9748e−07
10^{-9}	4.8526e−03	6.4664e−05	6.9750e−07
10^{-10}	4.8524e−03	6.4661e−05	6.9749e−07

To assess the *robustness of the energy-norm errors* with respect to the singular perturbation parameter ε, we fix the mesh size at $N = 128$ and systematically vary ε over the range $10^{-2} \leq \varepsilon \leq 10^{-10}$. The results, summarized in Table 2, demonstrate that the computed energy-norm errors remain essentially uniform across the entire range of ε. By "robustness," we mean that the error magnitude is largely insensitive to the decreasing values of ε, indicating that the proposed numerical scheme accurately

captures both the smooth and boundary-layer components of the solution without any deterioration in accuracy as $\varepsilon \to 0$. This behavior confirms the theoretical predictions of uniform convergence with respect to the singular perturbation parameter and highlights the method's reliability for extremely small values of ε.

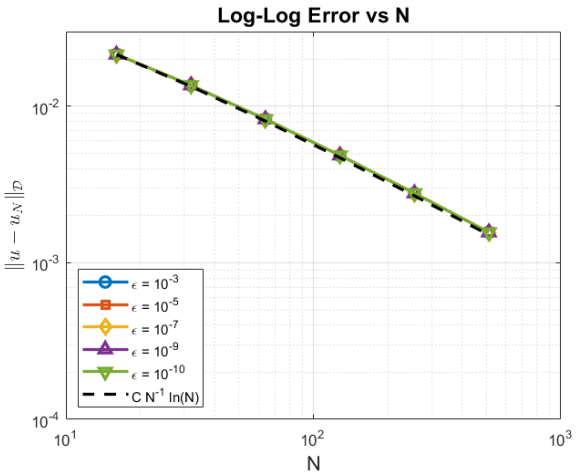

(a) Log-log plot for $\mathbb{P}_2$ element

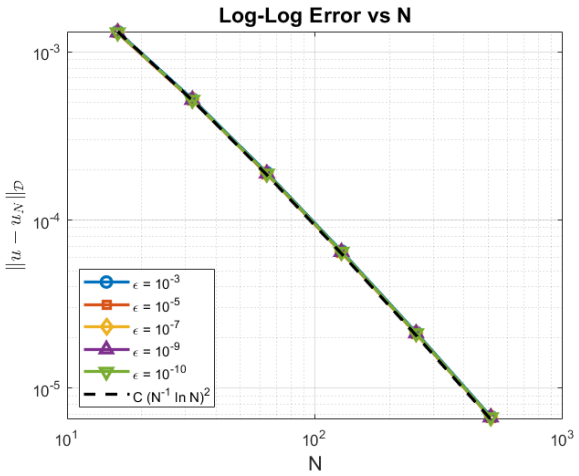

(b) Log-log plot for $\mathbb{P}_3$ element

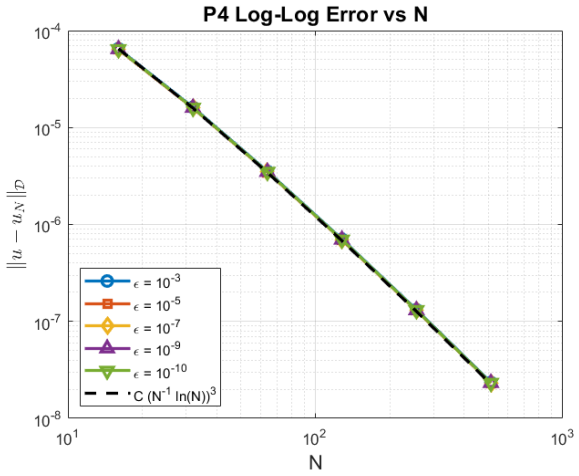

(c) Log-log plot for $\mathbb{P}_4$ element

Figure 2. The order of convergence in the energy-norm on the Shishkin mesh with $\mathbb{P}_2$, $\mathbb{P}_3$ and $\mathbb{P}_4$ elements for various values of ε.

Figure 2 illustrates the convergence behavior of the numerical solution in terms of the error versus the mesh size N on a log-log scale for Example 6.1. The slopes of the curves indicate the effective convergence rates. As observed, the numerical errors decrease approximately as follows

$$\|v - v_N\|_{\mathcal{D}} \sim \left(N^{-1} \ln N\right)^{r-1}.$$

This demonstrates that the convergence rate increases with the polynomial degree, and the numerical results closely match the theoretical predictions.

Moreover, for smaller values of the singular perturbation parameter ε, the errors approach an asymptotic regime, exhibiting ε-uniform behavior consistent with the limit $\varepsilon \to 0$. These observations

confirm the robustness and accuracy of the method across different mesh resolutions and perturbation parameters, providing strong numerical evidence in support of the theoretical error estimates.

Table 3. Comparison of the energy norm errors on uniform and Shishkin meshes with $N = 128$ for $\mathbb{P}_2$, $\mathbb{P}_3$, and $\mathbb{P}_4$ elements, for different values of the perturbation parameter ε.

	Shishkin mesh			Uniform mesh		
ε	$k = 2$	$k = 3$	$k = 4$	$k = 2$	$k = 3$	$k = 4$
10^{-2}	4.86e−03	6.54e−05	7.05e−07	8.31e−03	1.42e−04	6.88e−06
10^{-4}	4.85e−03	6.42e−05	6.92e−07	2.28e−02	8.40e−03	1.75e−04
10^{-6}	4.85e−03	6.46e−05	6.96e−07	1.69e−02	1.41e−02	1.20e−02
10^{-8}	4.85e−03	6.47e−05	6.97e−07	1.68e−02	1.69e−02	1.69e−02
10^{-10}	4.85e−03	6.47e−05	6.97e−07	1.68e−02	1.69e−02	1.69e−02

Table 3 presents a comparison of the energy norm errors obtained on Shishkin and uniform meshes for different values of the perturbation parameter ε. It is clearly observed that the errors on the Shishkin mesh remain essentially constant as ε decreases, indicating that the method exhibits ε-uniform convergence.

In contrast, the results on the uniform mesh deteriorate significantly as ε becomes small. In particular, for $\varepsilon \leq 10^{-6}$, the errors increase substantially and eventually stagnate, demonstrating the inability of the uniform mesh to resolve the boundary layers present in the solution. This behavior is consistent across all polynomial degrees.

Moreover, while higher-order elements ($k = 3, 4$) improve the accuracy for moderate values of ε, their advantage diminishes on uniform meshes for very small values of ε, where all methods exhibit similar error levels. This further highlights that mesh adaptation, rather than polynomial degree alone, is essential for achieving robust and accurate approximations in singularly perturbed problems.

These results clearly demonstrate the necessity of layer-adapted meshes for fourth-order singularly perturbed problems. The Shishkin mesh successfully captures the boundary layer behavior and delivers robust, ε-uniform accuracy, whereas the uniform mesh fails to do so, regardless of the polynomial degree used. This confirms the effectiveness of the proposed numerical strategy when combined with appropriate mesh design.

Example 6.2. *Consider the following linear variable coefficient boundary value problem:*

$$\varepsilon\, v^{(4)}(x) - e^{(1-x)}v'''(x) - v''(x) + (3 + x)v'(x) + 2v(x) = e^x, \quad 0 \leq x \leq 1, \tag{99}$$

subject to the boundary conditions

$$v(0) = v(1) = v'(0) = v''(1) = 0.$$

The exact solution of (99) *is unknown. Figure 3 illustrates the numerical solutions v_N and the discrete second derivative $D_w^2 v_N$ obtained using the WG-FEM on a Shishkin mesh, for $\varepsilon = 10^{-2}$ and $\varepsilon = 10^{-4}$ and using $\mathbb{P}_3$ element and $N = 128$ intervals.*

To estimate the order of convergence, we use the double mesh principle [23]. Specifically, we calculate the error $\|v_{2N} - v_N\|_{\mathcal{D}}$, where v_{2N} denotes the WG-FEM solution on a refined Shishkin mesh obtained by introducing the midpoints of the original mesh.

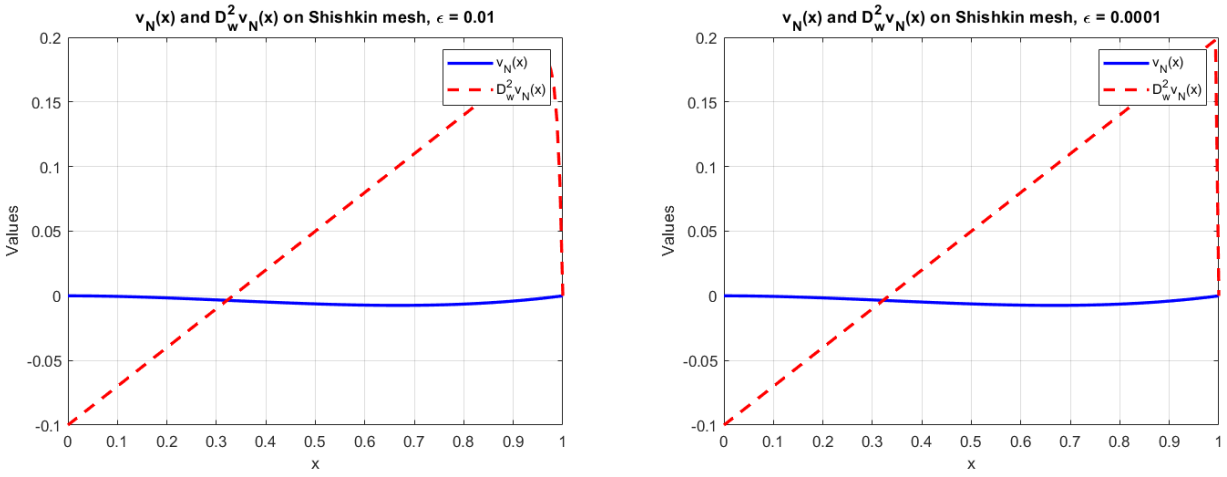

(a) WG solution for $\varepsilon = 10^{-2}$

(b) WG solution for $\varepsilon = 10^{-4}$

Figure 3. The WG-FEM solutions on the Shishkin mesh with $\mathbb{P}_3$ for $N = 256$.

Table 4. The errors in the energy norm and OC for the values of $\varepsilon = 10^{-2}$,10^{-4}, and 10^{-8}.

		10^{-2}		10^{-4}		10^{-8}	
	N	$\|\|v_{2N} - v_N\|\|_{\mathcal{D}}$	OC	$\|\|v_{2N} - v_N\|\|_{\mathcal{D}}$	OC	$\|\|v_{2N} - v_N\|\|_{\mathcal{D}}$	OC
	16	6.3282e−03	-	6.3284e−03	-	6.3279e−03	-
	32	4.0481e−03	0.960	4.0323e−03	0.963	4.0437e−03	0.962
	64	2.4347e−03	0.975	2.4178e−03	0.978	2.3852e−03	0.976
$\mathbb{P}_2$	128	1.4339e−03	0.985	1.4235e−03	0.988	1.4058e−03	0.986
	256	8.2114e−04	0.992	8.1496e−04	0.993	8.0543e−04	0.993
	512	4.6268e−04	0.998	4.5735e−04	0.999	4.5297e−04	0.998
	16	9.8401e−04	-	9.9013e−04	-	9.9031e−04	-
	32	4.1285e−04	1.848	4.1112e−04	1.870	4.1096e−04	1.871
	64	1.5217e−04	1.954	1.5189e−04	1.949	1.5203e−04	1.946
$\mathbb{P}_3$	128	5.4302e−05	1.912	5.4226e−05	1.911	5.4241e−05	1.912
	256	1.7904e−05	1.982	1.7931e−05	1.977	1.7918e−05	1.979
	512	5.6912e−06	1.992	5.6924e−06	1.994	5.6936e−06	1.992
	16	5.6761e−05	-	5.6139e−05	-	5.6162e−05	-
	32	1.4193e−05	2.948	1.4297e−05	2.953	1.4098e−05	2.945
	64	3.1047e−06	2.974	3.1194e−06	2.978	3.0896e−06	2.972
$\mathbb{P}_4$	128	6.2114e−07	2.987	6.2488e−07	2.988	6.1792e−07	2.982
	256	1.1903e−07	2.950	1.1997e−07	2.955	1.1798e−07	2.948
	512	2.1904e−08	2.942	2.1995e−08	2.948	2.1796e−08	2.940

For the second example, we report the error measurements and investigate the corresponding OC in the energy norm for the perturbation parameters $\varepsilon = 10^{-2}, 10^{-4}$, and 10^{-8}, as presented in Table 4. The results demonstrate that the observed convergence rates align closely with the theoretical predictions

given in Theorem 5.3, thereby providing further numerical confirmation of the established error bounds.

Figure 4 illustrates the convergence behavior of the numerical solution for Example 6.2 on a Shishkin mesh, plotting the error versus the mesh size N on a log-log scale. The slopes of the curves indicate that the convergence behaves in a manner similar to that observed in Example 6.1, with the errors decreasing approximately as

$$\|v - v_N\|_{\mathcal{D}} \sim (N^{-1} \ln N)^{r-1}.$$

This demonstrates that the numerical results remain consistent with the theoretical predictions, as previously observed.

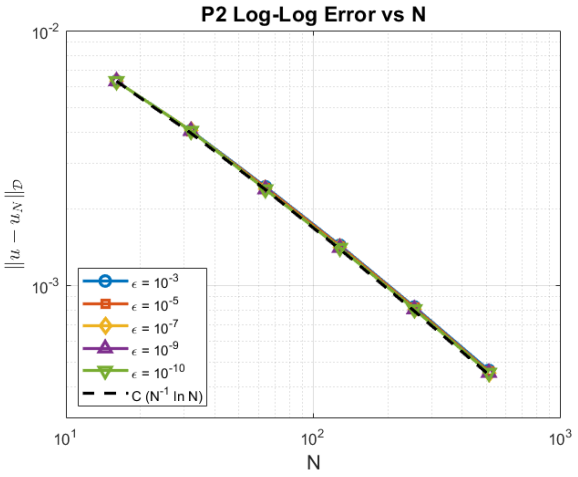

(a) Log-log plot for $\mathbb{P}_2$ element.

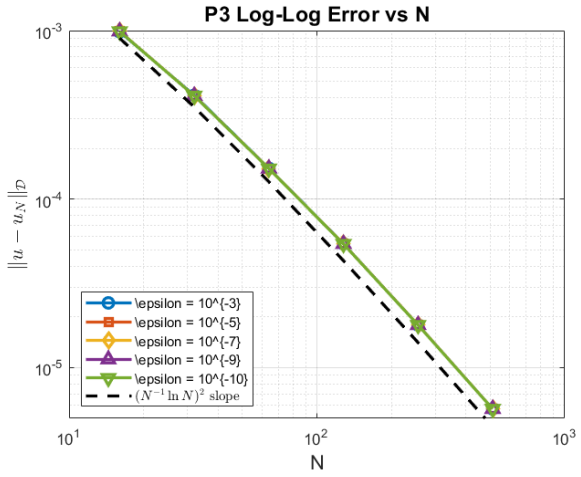

(b) Log-log plot for $\mathbb{P}_3$ element.

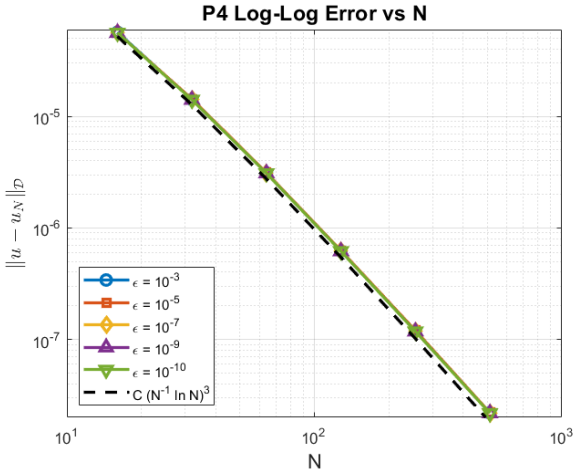

(c) Log-log plot for $\mathbb{P}_4$ element.

Figure 4. The order of convergence in the energy-norm of Example 6.2 on the Shishkin mesh with $\mathbb{P}_2$, $\mathbb{P}_3$, and $\mathbb{P}_4$ elements for various values of ε.

The results presented in Table 5 demonstrate the robustness of the computed energy errors with respect to the singular perturbation parameter ε. Specifically, for each polynomial degree $\mathbb{P}_2$, $\mathbb{P}_3$, and $\mathbb{P}_4$, the errors remain essentially unchanged across a wide range of values ε from 10^{-2} to 10^{-10}. The small

variations introduced for the intermediate values of ε illustrate that the numerical method produces stable and consistent results even as the parameter approaches zero, which confirms the theoretical predictions of uniform convergence. This robustness indicates that the discretization scheme is reliable for singularly perturbed problems and that the accuracy of the solution is not sensitive to the magnitude of ε.

Table 5. The energy errors using $N = 128$ and $\mathbb{P}_2$, $\mathbb{P}_3$, and $\mathbb{P}_4$ elements for various values of ε.

ε	$\mathbb{P}_2$	$\mathbb{P}_3$	$\mathbb{P}_4$
10^{-2}	1.4339e−03	6.0302e−05	6.2114e−07
10^{-3}	1.4241e−03	6.0210e−05	6.2120e−07
10^{-4}	1.4235e−03	6.0105e−05	6.2488e−07
10^{-5}	1.4218e−03	6.0102e−05	6.2493e−07
10^{-6}	1.4216e−03	6.0109e−05	6.2489e−07
10^{-7}	1.4107e−03	6.0111e−05	6.2091e−07
10^{-8}	1.4058e−03	6.0501e−05	6.1792e−07
10^{-9}	1.4059e−03	6.0503e−05	6.1793e−07
10^{-10}	1.4057e−03	6.0499e−05	6.1791e−07

7. Conclusions

In this work, we have applied the WG-FEM to fourth-order singularly perturbed boundary value problems with boundary layers. By utilizing Shishkin meshes, the numerical method is able to resolve sharp boundary layers efficiently while maintaining high accuracy in the interior domain.

The numerical experiments for various examples demonstrate that the WG-FEM achieves the theoretically predicted convergence rates in the energy norm. In particular, the method exhibits optimal convergence up to a logarithmic factor when higher-order polynomial elements are used, and the numerical solutions accurately capture both the smooth behavior in the interior and the steep gradients near the boundary.

Moreover, the results confirm that the convergence behavior on Shishkin meshes is robust with respect to the singular perturbation parameter ε, and the method remains stable even for very small values of ε. Overall, the study illustrates that the WG-FEM combined with layer-adapted meshes provides an effective and reliable approach for solving high-order singularly perturbed problems of the convection type. Future work could explore an extension to multi–dimensional problems and an application to time-dependent singularly perturbed equations.

Use of AI tools declaration

The authors declare they have not used artificial intelligence (AI) tools in the creation of this article.

Conflict of interest

The authors declare there is no conflicts of interest.

References

1. H. G. Roos, M. Stynes, L. Tobiska, *Robust Numerical Methods for Singularly Perturbed Differential Equations*, 2^{nd} edition, in *Springer Series in Computational Mathematics*, Springer Berlin, Heidelberg, **24** (2008). https://doi.org/10.1007/978-3-540-34467-4
2. T. Linß, Layer-adapted meshes for convection–diffusion problems, *Comput. Methods Appl. Mech. Eng.*, **192** (2003), 1061–1105. https://doi.org/10.1016/S0045-7825(02)00630-8
3. M. Stynes, D. Stynes, *Convection–Diffusion Problems: An Introduction to Their Analysis and Numerical Solution*, in Graduate Studies in Mathematics, American Mathematical Society, 2018. https://doi.org/10.1090/gsm/196
4. B. Semper, Conforming finite element approximations for a fourth-order singular perturbation problem, *SIAM J. Numer. Anal.*, **29** (1992), 1043–1058. https://doi.org/10.1137/0729063
5. G. F. Sun, M. Stynes, Finite-element methods for singularly perturbed high-order elliptic two-point boundary value problems. I: Reaction-diffusion-type problems, *IMA J. Numer. Anal.*, **15** (1995), 117–139. https://doi.org/10.1093/imanum/15.1.117
6. H. Guo, C. Huang, Z. Zhang, Superconvergence of conforming finite element for fourth-order singularly perturbed problems of reaction-diffusion type in one dimension, *Numer. Methods Partial Differ. Equations*, **30** (2014), 550–566. https://doi.org/10.1002/num.21827
7. X. Meng, M. Stynes, Convergence analysis of the Adini element on a Shishkin mesh for a singularly perturbed fourth-order problem in two dimensions, *Adv. Comput. Math.*, **45** (2019), 1105–1128. https://doi.org/10.1007/s10444-018-9646-0
8. S. Franz, H. Roos, Robust error estimation in energy and balanced norms for singularly perturbed fourth-order problems, *Comput. Math. Appl.*, **72** (2016), 233–247. https://doi.org/10.1016/j.camwa.2016.05.001
9. Y. Liu, Y. Cheng, Local discontinuous Galerkin method for a singularly perturbed fourth-order problem of reaction-diffusion type, *J. Comput. Appl. Math.*, **440** (2024), 115641. https://doi.org/10.1016/j.cam.2023.115641
10. G. F. Sun, M. Stynes, Finite-element methods for singularly perturbed high-order elliptic two-point boundary value problems. II: convection–diffusion-type problems, *IMA J. Numer. Anal.*, **15** (1995), 197–219. https://doi.org/10.1093/imanum/15.2.197
11. V. Shanthi, N. Ramanujam, Asymptotic numerical methods for singularly perturbed fourth-order ordinary differential equations of convection–diffusion type, *Appl. Math. Comput.*, **133** (2002), 559–579. https://doi.org/10.1016/S0096-3003(01)00257-0
12. S. Singh, D. Kumar, V. Shanthi, Uniformly convergent scheme for fourth-order singularly perturbed convection–diffusion ODE, *Appl. Numer. Math.*, **186** (2023), 334–357. https://doi.org/10.1016/j.apnum.2023.01.020
13. J. Wang, X. Ye, A weak Galerkin finite element method for second-order elliptic problems, *J. Comput. Appl. Math.*, **241** (2013), 103–115. https://doi.org/10.1016/j.cam.2012.10.003
14. Q. Guan, W. Zhao, Error analysis of energy stable weak Galerkin schemes for the Allen-Cahn equation, *Adv. Comput. Sci. Eng.*, **7** (2026), 48–72. https://doi.org/10.3934/acse.2026003

15. W. Zhao, Q. Guan, Numerical analysis of energy stable weak Galerkin schemes for the Cahn-Hilliard equation, *Commun. Nonlinear Sci. Numer. Simul.*, **118** (2023), 106999. https://doi.org/10.1016/j.cnsns.2022.106999
16. Ş. Toprakseven, Optimal order uniform convergence of weak Galerkin finite element method on Bakhvalov-type meshes for singularly perturbed convection dominated problems, *Hacet. J. Math. Stat.*, **52** (2023), 850–875. https://doi.org/10.15672/hujms.1117320
17. S. Toprakseven, N. Srinivasan, An efficient weak Galerkin FEM for third-order singularly perturbed convection–diffusion differential equations on layer-adapted meshes, *Appl. Numer. Math.*, **204** (2024), 130–146. https://doi.org/10.1016/j.apnum.2024.06.009
18. S. Toprakseven, S. Dinibutun, A weak Galerkin finite element method for parabolic singularly perturbed convection–diffusion equations on layer-adapted meshes, *Electron. Res. Arch.*, **32** (2024), 5033–5066. https://doi.org/10.3934/era.2024232
19. E. C. Gartland, Graded-mesh difference schemes for singularly perturbed two-point boundary value problems, *Math. Comput.*, **51** (1988), 631–657. https://doi.org/10.1090/S0025-5718-1988-0935072-1
20. P. Zhu, S. Xie, A uniformly convergent weak Galerkin finite element method on Shishkin mesh for one-dimensional convection–diffusion problems, *J. Sci. Comput.*, **85** (2020), 34. https://doi.org/10.1007/s10915-020-01345-3
21. D. A. Di Pietro, A. Ern, *Mathematical Aspects of Discontinuous Galerkin Methods*, Springer Science & Business Media, 2011. https://doi.org/10.1007/978-3-642-22980-0
22. L. Yan, Z. Wang, Y. Cheng, Local discontinuous Galerkin method for a third-order singularly perturbed problem of convection–diffusion type, *Comput. Methods Appl. Math.*, **23** (2023), 751–766. https://doi.org/10.1515/cmam-2022-0176
23. P. Farrell, A. Hegarty, J. M. Miller, E. O'Riordan, G. I. Shishkin, *Robust Computational Techniques for Boundary Layers*, Chapman and Hall/CRC, 2000.

AIMS Press